A MESOSCALE INVESTIGATION OF CONVECTIVE ACTIVITY

by

Leo Harvey Craiglow

United States
Naval Postgraduate School

THESIS

A MESOSCALE INVESTIGATION OF

CONVECTIVE ACTIVITY

by

Leo Harvey Craiglow, Jr.

Thesis Advisor: R. L. Alberty

March 1971

Approved for public release; distribution unlimited.

A Mesoscale Investigation of Convective Activity

by

Leo Harvey Craiglow, Jr.
Lieutenant Commander, United States Navy
A.B., University of Rochester, 1961

Submitted in partial fulfillment of the
requirements for the degree of

MASTER OF SCIENCE IN METEOROLOGY

from the

NAVAL POSTGRADUATE SCHOOL
March 1971

ABSTRACT

A mesoscale investigation of a series of tornadoes and thunderstorms that passed through the NSSL mesonetwork in Oklahoma, on 10 June 1967, between 1700 and 2300 CST, was conducted. Utilizing upper air data provided by NSSL, the divergence, vertical motion, and energy fields were computed.

A finite-difference technique for computing and smoothing divergence was developed. The vertical motion was then computed by means of the kinematic method. Both the total derivative and the local rate of change of static energy were computed. Using the values of the local rate of change, prognostic fields of static energy and an energy index were obtained. Finally, forecast energy indexes, divergence, and vertical motion fields were compared to the observed locations of tornadoes and thunderstorms.

TABLE OF CONTENTS

LIST OF FIGURES

TABLE OF SYMBOLS AND ABBREVIATIONS

A	Area computed using trapezoidal rule
c_n	Normal component of the wind at a boundary
C_p	Specific heat at constant pressure
CST	Central Standard Time
DIV	Divergence
DVERT	Divergence error term
E.I.	Energy Index
E_s	Static energy
E_T	Total energy
F	Frictional heating
g	Acceleration of gravity
GMT	Greenwich Meridian Time
h	Sum of sensible heat, evaporation, and radiation
L	Latent heat
P	Pressure in millibars
q	Specific humidity
T	Temperature
T_d	Dewpoint temperature
u	Component of $\vec{V}$ in x direction
v	Component of $\vec{V}$ in y direction
$\vec{V}$	Horizontal wind velocity
V	Scalar velocity
w	Mixing ratio
Z	Vertical height
α	Specific volume

ω	Vertical component of wind (x,y,p,t) system
δl	Incremental length along the side of a boundary
∇	Isobaric del operator
∇_h	Horizontal cartesian del operator
$\nabla \cdot \vec{V}$	Isobaric divergence, also abbreviated by DIV
$\widetilde{\nabla \cdot \vec{V}_2}$	Area averaged isobaric divergence
$\widehat{\nabla \cdot \vec{V}}$	Vertically averaged isobaric divergence
$\vec{V} \cdot \nabla_h p_{sfc}$	Terrain effect
θ_E	Equivalent potential temperature

TABLE OF SYMBOLS AND ABBREVIATIONS

A	Area computed using trapezoidal rule
c_n	Normal component of the wind at a boundary
C_p	Specific heat at constant pressure
CST	Central Standard Time
DIV	Divergence
DVERT	Divergence error term
E.I.	Energy Index
E_s	Static energy
E_T	Total energy
F	Frictional heating
g	Acceleration of gravity
GMT	Greenwich Meridian Time
h	Sum of sensible heat, evaporation, and radiation
L	Latent heat
P	Pressure in millibars
q	Specific humidity
T	Temperature
T_d	Dewpoint temperature
u	Component of $\vec{V}$ in x direction
v	Component of $\vec{V}$ in y direction
$\vec{V}$	Horizontal wind velocity
V	Scalar velocity
w	Mixing ratio
Z	Vertical height
α	Specific volume

ω	Vertical component of wind (x,y,p,t) system
δl	Incremental length along the side of a boundary
∇	Isobaric del operator
∇_h	Horizontal cartesian del operator
$\nabla \cdot \vec{V}$	Isobaric divergence, also abbreviated by DIV
$\widetilde{\nabla \cdot \vec{V}_2}$	Area averaged isobaric divergence
$\overbrace{\nabla \cdot \vec{V}}$	Vertically averaged isobaric divergence
$\vec{V} \cdot \nabla_h p_{sfc}$	Terrain effect
θ_E	Equivalent potential temperature

ACKNOWLEDGEMENTS

The author wishes to take this opportunity to express his appreciation to his advisor, Professor R. L. Alberty, for his support, suggestions, advice, assistance, and guidance through the many pitfalls encountered in this research.

Appreciation is also expressed to Professor J. D. Mahlman, presently on leave of absence from the Naval Postgraduate School, who initially started the author on the long winding road that has ultimately led to the completion of this thesis.

To the National Severe Storms Laboratory (NSSL) for providing the computerized data, to Mr. P. L. Adler of the Meteorology Department for his assistance in plotting the original NSSL data, and to the W. R. Church Computer Facility of the Naval Postgraduate School for the free use of the IBM 360 Computer, my heartfelt thanks.

Finally, a special note of gratitude and deepest appreciation goes to my wife, who besides being a companion, gave me the strength to persevere and stood by me during the darkest hours before the dawn. Without her understanding and love, plus keeping the children out of my hair, this thesis would never have reached fruition.

I. INTRODUCTION

Research in meteorology is normally related to one or more of three general scales of atmospheric motion. Although most meteorologists accept the division of the atmosphere into three scales of motion, they do not agree as to the exact definitions and dividing lines between these scales. The Glossary of Meteorology (1959) defined these scales as:

1. Synoptic or cyclonic meteorology, which refers to the migratory high and low pressure systems of the lower troposphere, with wave lengths of 1000 to 2500 kilometers;
2. Mesometeorology, which is concerned with the detection and analysis of the types of major weather phenomena that are small enough to remain undetected within a normal observation network;[1] and
3. Micrometeorology, which deals with the observations and explanations of the smallest-scale physical and dynamic occurrences within the atmosphere and is normally confined to the surface boundary layer of the atmosphere.

The majority of meteorological research performed has been done on the synoptic scale due to the world-wide synoptic network of surface and upper air reporting stations.

---

[1] Fiedler and Panofsky (1970) defined the wavelengths for the mesoscale as lying between 20 and 500 kilometers.

In addition, a large amount of research has been undertaken on the micrometeorological scale with researchers being able to set up dense surface networks to investigate areas even smaller than one square kilometer without excessive difficulty.

It is in the area of mesometeorology that research has lagged. This has been primarily due to the fact that the synoptic data network is not dense enough, even in the United States, to allow adequate resolution of such weather phenomena as tornadoes and thunderstorms. As a result, early mesoscale investigators, such as Fujita (1955) who investigated a system of squall lines in the central United States, were forced to use synoptic data. Fujita attempted to overcome the inadequacy of the synoptic data by converting time cross sections to space cross sections. Nevertheless, Fujita noted that mesoscale networks were essential if research in mesometeorology was to advance.

Due to the efforts of Fujita and others, a surface mesonetwork was established in central Oklahoma by the National Severe Storms Project (NSSP) in the spring of 1960. This network, referred to as the Beta network, was established in order to obtain data on the severe thunderstorms and tornadoes which are prevalent in central Oklahoma in the spring. Although the network consisted of some 36 reporting stations located from 10 to 15 miles apart, it was evident that a knowledge of surface conditions was not sufficient.

Finally, in 1966, the National Severe Storms Laboratory (NSSL) of the Environmental Sciences Service Administration

(ESSA) augmented the Beta network with a nine station upper-air mesonetwork covering south-central Oklahoma. The nine stations, located from 40 to 50 miles apart in 1966 and 1967, took upper-air soundings every 90 minutes during periods of strong convective activity in the spring and early summer. This resulted in greater in-depth analysis of mesoscale phenomena over more extended periods of time than previously possible.

In 1968, NSSL relocated the nine stations such that the distance between them was approximately one-half what it was previously. This resulted in a more dense upper-air reporting network, but at the sacrifice of reducing the area available for investigation. In 1970, ESSA became a department under the National Oceanic and Atmospheric Administration (NOAA).

The inherent errors contained in present day radiosondes have led to questions concerning the reliability of the data obtained from the more dense network. As a result, some researchers have limited themselves to the extensive data obtained by NSSL during 1966 and 1967 for detailed studies of severe storms and their associated weather phenomena. One such set of data was used for this study.

On 10 June 1967, convective activity was present throughout the NSSL network. As described in Storm Data (1967), this convective activity resulted in scattered but frequent tornadoes, thunderstorms, hail, high winds, and heavy rains during the observation period from 1700 CST through 2300 CST on 10 June 1967 (2300 GMT, 10 June 1967 through 0500 GMT, 11

June 1967). Indicative of the severity of this weather is the following report contained in Storm Data (1967), for the central part of Blaine County, Oklahoma, between 1930 CST and 2200 CST, on 10 June 1967:

> "Heavy thunderstorms moving northeastward across the County caused heavy wind damage in the Hitchcock-Watonga-Greenfield area. One tornado was observed on the northwest side of Watonga about 8:30 pm. Three other funnels aloft were sighted near the city and may have possibly passed low over the city during the blinding rain. A 1/3 mile-path in the Hillcrest Heights addition in northwest Watonga left a demolished hanger and five smashed airplanes, 2 homes completely destroyed, 8 homes with extensive damage, and most others damaged to some extent in the city. Roofs of downtown businesses were damaged and windows blown out. Three trailer homes were demolished. A second tornado is believed to have struck the OG&E transformer station 6 miles east of Watonga because the 30 tons of steel structure was lifted up into the air and dropped 150 feet to the east. Nearly every farm homestead in the area received heavy outbuilding damage and some lost homes and heavy steel buildings."

Because of the intensity of such storms and the damage caused by them, it is imperative that research be continued in meso-meteorology.

In order to investigate atmospheric phenomena occurring on the mesoscale, a 12X10 grid was superimposed on the NSSL network encompassing an area from 96°45' to 99°30' West and from 33°45' to 36°00' North, in grid sections of 15' longitude and latitude respectively. Figure 1 shows the overall grid with the dashed lines enclosing the reduced grid area utilized for most computations in this study due to the finite differencing schemes employed.

Utilizing the data for the five time frames commencing with 2300 GMT, 10 June 1967, and spaced 90 minutes apart, this study attempted to:

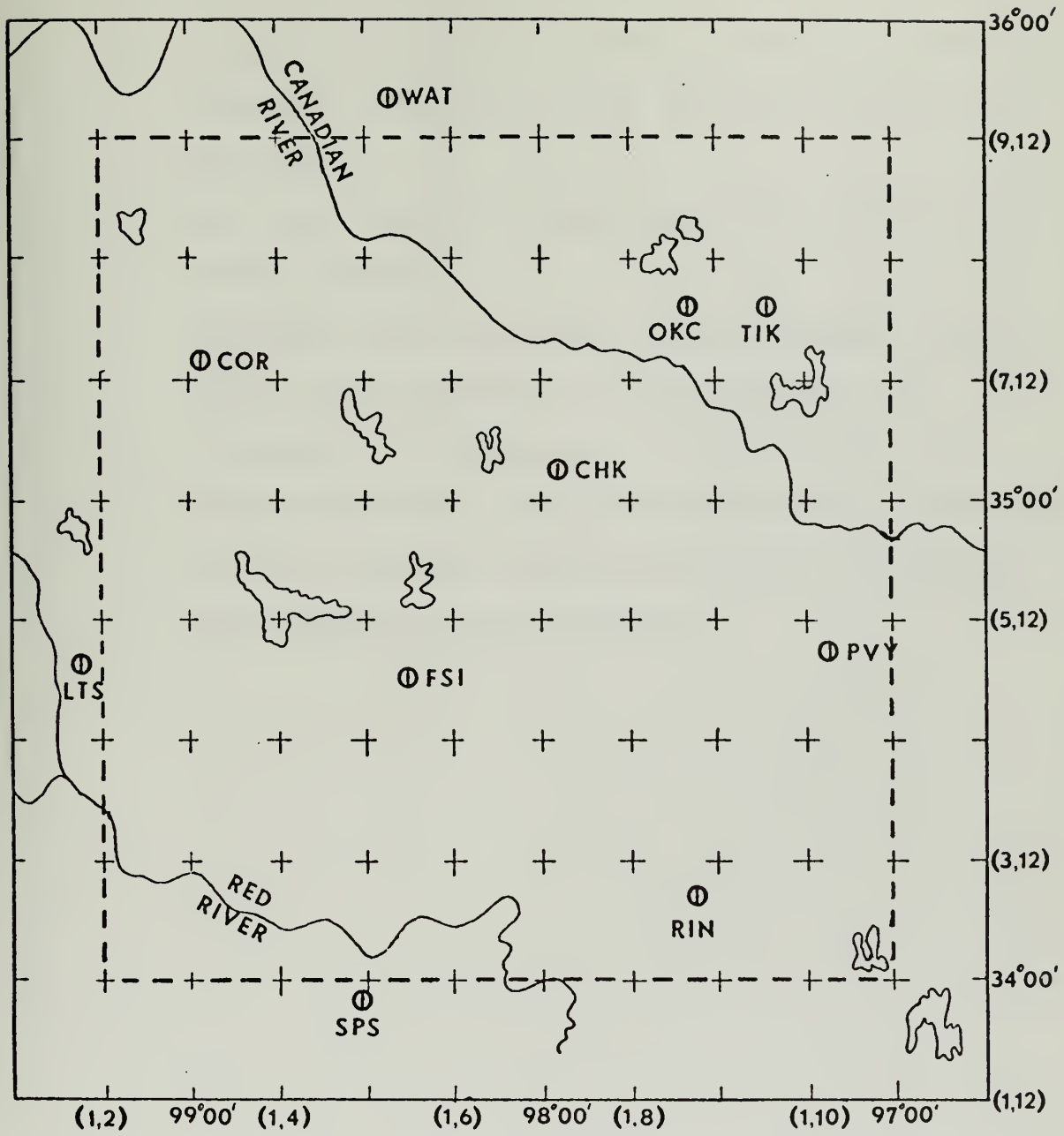

Fig. 1. Mesoscale grid network used in study. Dashed line encloses area utilized for most computations. Upper air reporting stations are indicated by ⊙.

1. Describe the overall convective activity occurring throughout the area during the period under investigation;
2. Develop a method for obtaining realistic vertical motion fields;
3. Determine what knowledge could be gained from the local rate of change of static energy; and
4. Correlate the divergence, vertical motion, and changes of static energy fields with the areas and times of tornadic activity in order to determine what mechanisms were present.

II. SYNOPTIC SITUATION AT 0000 GMT, 11 June 1967

To aid in understanding what has occurred on the mesoscale, it is helpful to look at the synoptic situation during the same time frame. During the period under investigation (2300 GMT, 10 June 1967 through 0500 GMT, 11 June 1967) a synoptic surface and upper air sounding in the NSSL network was taken at 0000 GMT, 11 June 1967, at Oklahoma City, Oklahoma. This sounding, which took place during the first hour of the time period, was taken at a time of marked tornado, thunderstorm, and hail occurrence in the northwestern section of the mesoscale network.

Figures 2 through 5 represent the synoptic situation over the south-central United States at 0000 GMT, 11 June 1967, as analyzed by the National Weather Service. Figure 2 details the surface situation. A stationary front was located in northwestern Texas and western Oklahoma, running in a northeasterly direction. A low pressure system with a weak wave in the front was present in the panhandle area of Texas. The wind ahead of the front was from the southeast bringing warm, relatively moist air from the Gulf of Mexico. This can be observed from the temperature and dewpoint temperatures plotted in Figure 2. The dewpoint temperatures behind the front were much lower, indicating warm dry air was advected behind the front from the deserts of New Mexico and Arizona. Since the temperatures on both sides of the front were comparable, the primary way to delineate the frontal location was by means of the wind shift across the front. In this case there

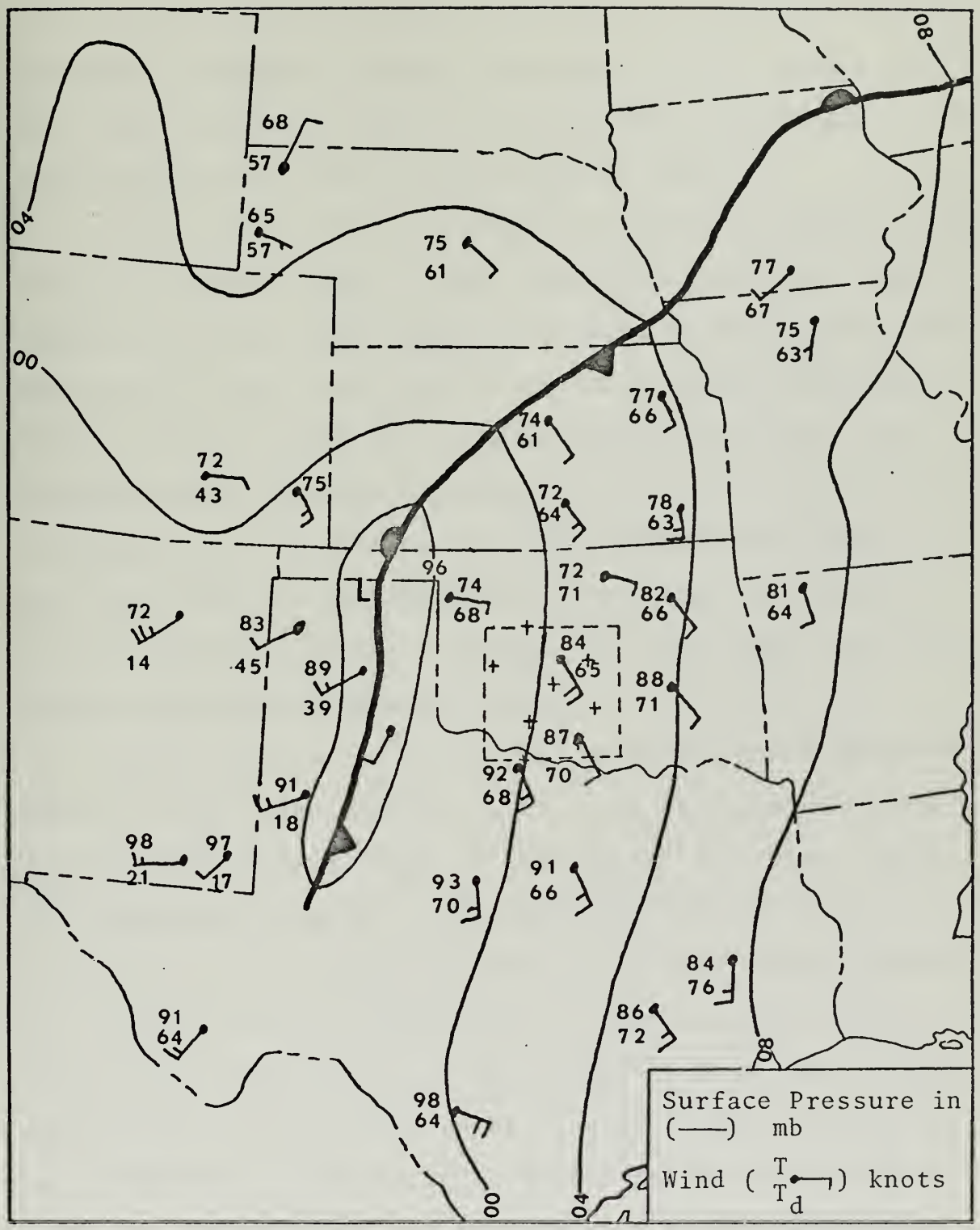

Fig. 2. Surface analysis for 0000 GMT, 11 June 1967, with stationary front. Dashed area indicates mesonetwork. T refers to the air temperature and T_d refers to dewpoint temperature, both in °F. Wind shafts indicate direction flow is from. Each full barb on the wind shaft represents 10 knots; half barbs represent 5 knots.

was a marked veering of the wind from the southeast to west-southwest, providing a clear indication of the front's location, and also indicating the presence of a low level convergence zone in the vicinity of the front.

Figure 3 outlines the synoptic situation at 850 mb. The front was still evident at this level with southerly flow advecting warm, moist air (mixing ratio of 10.0 g/kg) into the area ahead of the front with westerly flow advecting warm, dry air (mixing ratio of 5.8 g/kg) behind the front. The isotherm pattern showed a definite influx of warm air into the mesonetwork area. The isoheight pattern was tightest over the center of the mesonetwork and indicated difluence in the northern section. Finally, the wind speed was relatively high over the mesonetwork.

Figure 4 shows the height and temperature patterns at 700 mb for the same area and time. The wind direction was from a southwesterly direction throughout the entire area. The temperature patterns indicated that warm air with a mixing ratio of 6.0 g/kg was advected into the NSSL network. This compared with a mixing ratio at the surface of 13.1 g/kg and at 850 mb of 13.5 g/kg, although some areas at the surface had mixing ratios as high as 15.0 g/kg. There was an indication of a convergence zone northeast of the mesonetwork. In addition, the maximum wind speed of 40 knots was recorded in the mesonetwork.

Figure 5 depicts the 500 mb height and temperature patterns. The wind, as at 700 mb, was predominately from the southwest; however, it was generally stronger than at 700 mb.

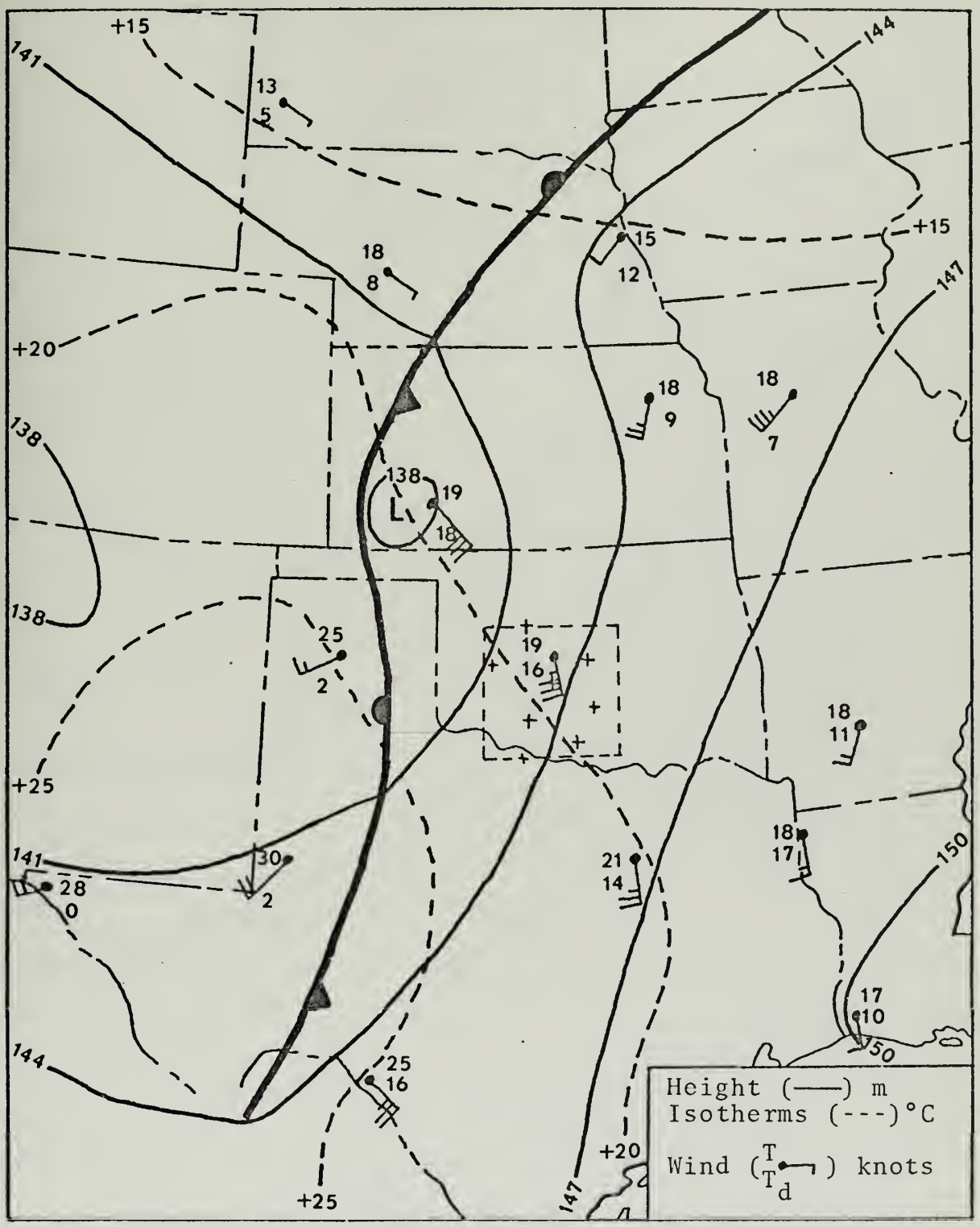

Fig. 3. 850 mb analysis for 0000 GMT, 11 June 1967, with height, isotherm, and frontal analysis. Dashed area indicates mesonetwork. T and T_d are expressed in °C.

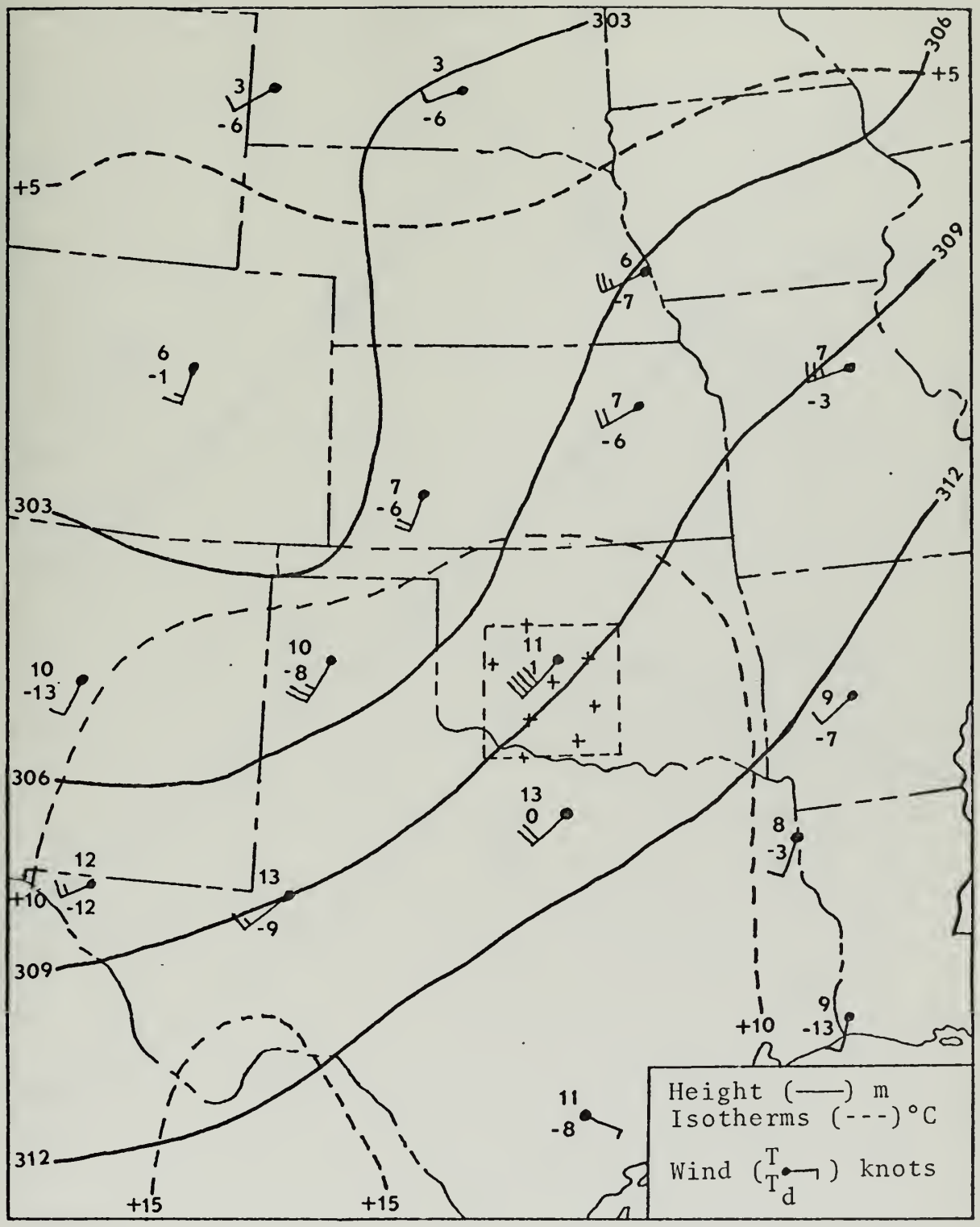

Fig. 4. 700 mb height and temperature analysis for 0000 GMT, 11 June 1967. Dashed area indicates mesonetwork. T and T_d are expressed in °C.

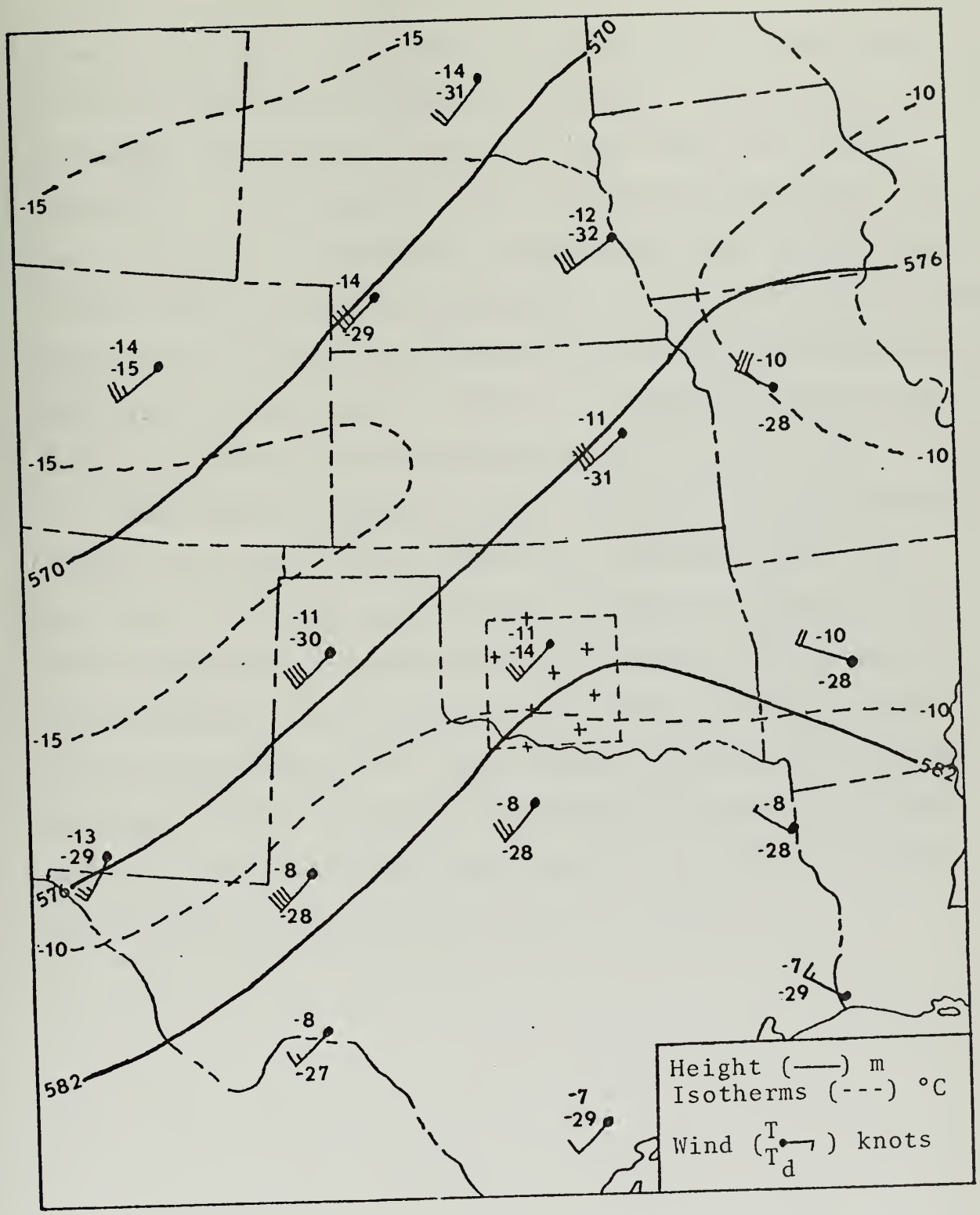

Fig. 5. 500 mb height and temperature analysis for 0000 GMT, 11 June 1967. Dashed area indicates mesonetwork. T and T_d are expressed in °C.

A weak ridge had formed over the central and eastern portions of Texas and southeastern Oklahoma. The mixing ratio throughout the general area was of the order of 0.7 g/kg. However, in the vicinity of the mesonetwork the mixing ratio was 2.5 g/kg. In addition, a convergence zone was indicated in the area of the mesonetwork where the wind speed decreased from 40 to 25 knots with a weak divergence zone to the northeast of the mesonetwork. Finally, a tongue of cold air was moving in toward the mesonetwork from the west.

The overall conclusion, based on these synoptic weather charts, was that in the vicinity of the mesonetwork, cold air with relatively high moisture values was located at 500 mb over warm air with high moisture values. This, coupled with the fact that convergence was indicated in the vicinity of the mesonetwork at all four levels, resulted in a highly unstable condition leading to convective overturning. The fact that severe weather was present in the mesonetwork at this time lends support to these conclusions.

III. INVESTIGATIVE PROCEDURES

A. DATA ANALYSIS

In order to accomplish the objectives of this study, it was necessary to analyze three parameters for each of the five sounding times (2300, 0030, 0200, 0330, and 0500 GMT) and 17 levels (surface to 150 mb at 50 mb intervals). Utilizing the computerized data provided by the NSSL mesonetwork for 10 June 1967, wind direction, wind speed, and static energy were plotted on the 17 isobaric surfaces for each of the nine stations for each time period.

A problem that developed in the plotting and analysis of the NSSL data was a combination of either the inability of some stations to launch a radiosonde due to severe weather conditions or, at some times, the radiosondes failing to reach the 150 mb level. This was especially true during the last three time periods when Watonga (WAT) failed to launch due to tornadoes and thunderstorms in the general vicinity. In addition, at 0330 GMT, Tinker (TIK) also failed to launch a radiosonde and Cordell's (COR) radiosonde only reached 350 mb. As a result, the northern section of the mesonetwork was almost entirely without reports necessitating subjective analysis based on extrapolation from previous times and from those reporting stations to the south. Unfortunately, all tornado and thunderstorm activity during the period of this study occurred north of a line from Cordell to Tinker. Therefore, the computed data for the important northern

section of the mesonetwork was obtained from extrapolated analyses and hence was subject to greater errors than the other sections.

Once all streamlines, isotach, and static energy patterns were analyzed, 120 data points were extracted for each level and time frame. In addition, a fourth parameter, surface pressure, was plotted and analyzed in order to take into account the surface effects upon the wind direction and speed. In all, 31,200 data points were extracted for the study.

In the case of all computed parameters, the centered finite differencing technique resulted in a reduced 10X8 grid. All parameters listed in this chapter are detailed in the computer program contained in Appendix A.

Space and time continuity were maintained throughout as consistently as possible. The continuity in space was facilitated by analyzing at 50 mb intervals which were chosen because the NSSL computerized data provided the information at these levels. Also, this allowed many small-scale motions to be picked out and analyzed that otherwise might have been missed if a larger vertical increment had been chosen.

All data was plotted and analyzed as on station data, even though in one case the launch times at the nine stations varied as much as 25 minutes. On the average the launch times varied only by nine minutes. In addition, the balloons obviously did not ascend in a straight vertical profile. Fankhauser (1969), felt that such factors as the lateral displacement of the balloon from its launch site, the variability of launch times, the differing rates of balloon ascent,

and the time lag of the different pressure levels from launch time must all be taken into account in performing mesoscale analysis. He felt that neglecting these factors would introduce extreme errors. To compensate for these factors, Fankhauser utilized a linear interpolation formula of the form

$$x = x_1 + \left(\frac{t - t_1}{t_2 - t_1} \right) (x_2 - x_1) \qquad (1)$$

where x is the variable under consideration and the subscripts 1 and 2 refer to adjacent soundings in time t.. This approach was investigated for use in this study, but it was decided not to use it for two reasons:

1. It approximately doubled the amount of data extraction required; and
2. It eliminated one time frame from utilization in the study.

B. DIVERGENCE COMPUTATIONS

Velocity divergence, which may be expressed as

$$DIV = \nabla \cdot \vec{V} = \frac{\partial u}{\partial x} + \frac{\partial v}{\partial y} \qquad (2)$$

was computed as it is a required parameter for any discussion of convective activity on the mesoscale where computation of vertical motion by the kinematic method is used.

A major problem in computing divergence is due to the fact that the individual terms are normally of approximately equal magnitude but of opposite sign. This results in the divergence being one order of magnitude smaller than the individual terms. This can result in large errors if either

the streamline and/or the isotach patterns are incorrectly analyzed, or if there is any error in the original data.

Although equation (1) was not utilized, it was realized that the points raised by Fankhauser were valid, at least to some extent. In order to compensate for the deviations previously listed, the divergence field was smoothed in both the horizontal and vertical.

The actual computation of isobaric divergence was done utilizing a centered, finite-difference, trapezoidal area-averaging technique based on Gauss' Theorem. It may be expressed as follows:

$$\widetilde{\nabla \cdot \vec{V}}_2 = - \frac{1}{A} \oint c_n \delta l \qquad (3)$$

where $\widetilde{\nabla \cdot \vec{V}}_2$ is the area-averaged isobaric divergence, A is the area computed using the trapezoidal rule, c_n is the normal component of the wind at the boundary, and δl is the incremental length along each side of the boundary. Figure 6 depicts a representation of the grid used. Area averaging in the horizontal succeeded in smoothing out many of the irregularities normally present in elementary divergence computations.

Once the divergence field had been smoothed in the horizontal, it was necessary to determine whether or not to smooth the divergence in the vertical. Computing divergence through all 17 levels with no vertical smoothing resulted in patterns as shown in Figure 7. In the case presented, the divergence pattern was not vertically consistent in that there were adjacent extremes of both convergence and divergence.

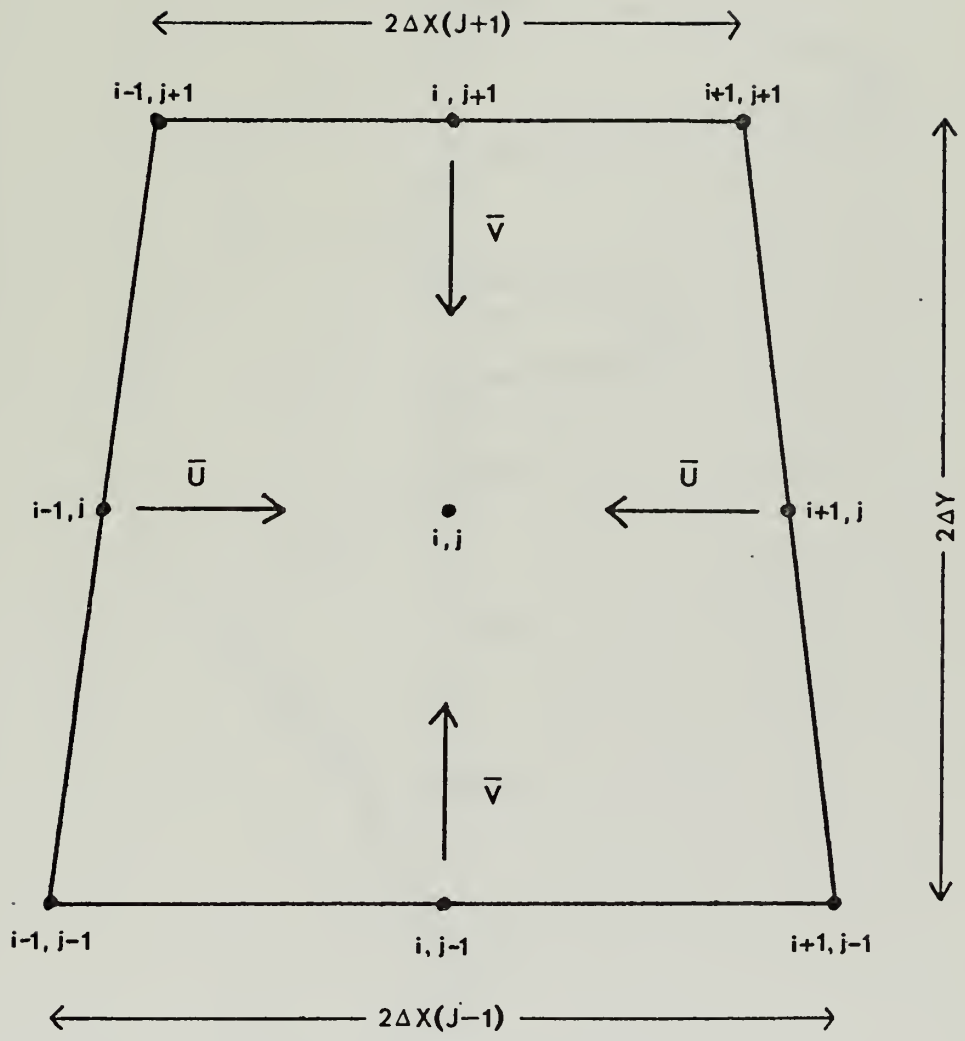

Fig. 6. Grid system used to compute divergence at any arbitrary interior point (i,j).

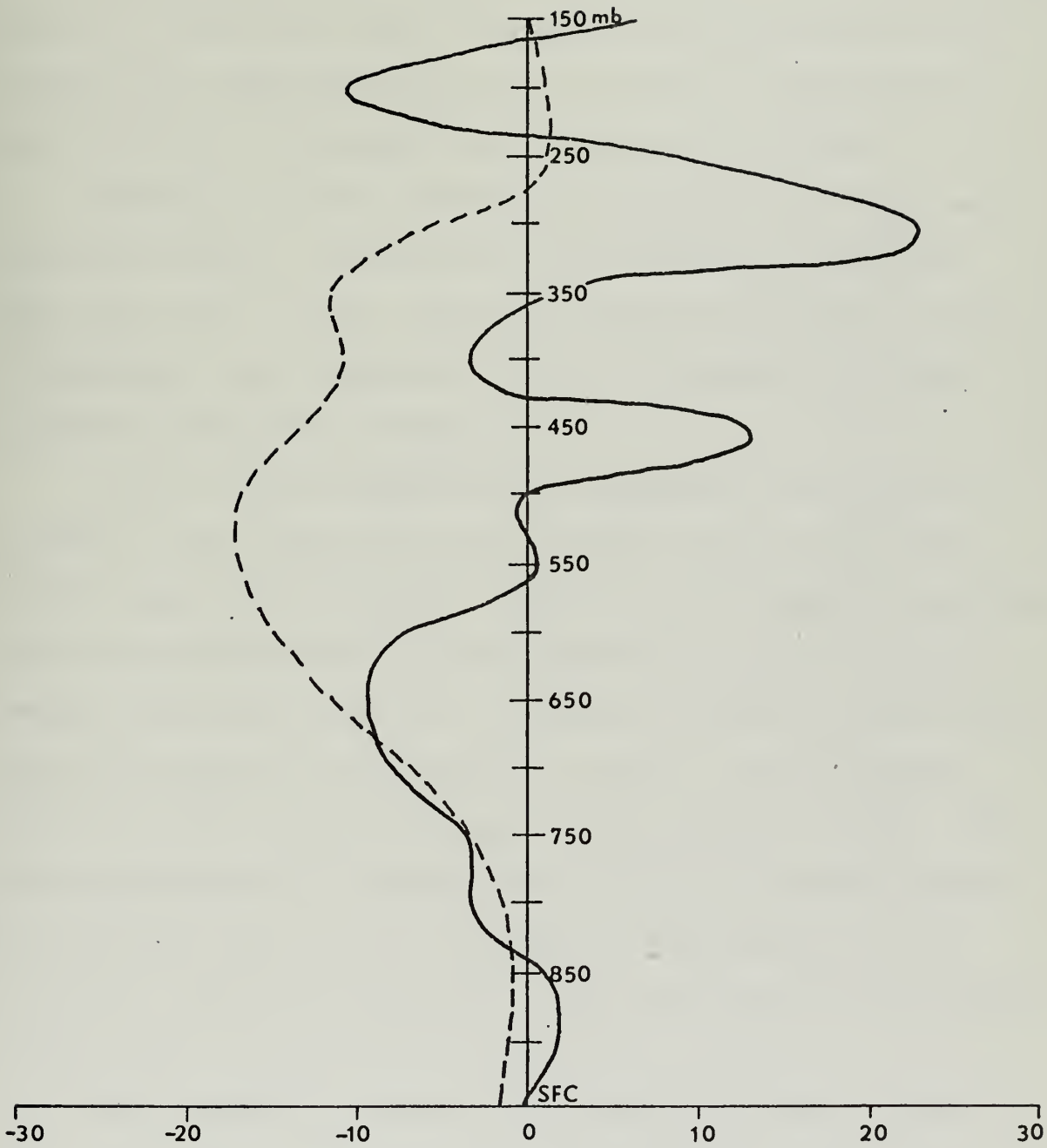

(——) Divergence $x10^5$ in units of sec^{-1}
(---) Vertical Motion $x10^3$ in units of mb sec^{-1}

Fig. 7. Divergence and vertical motion for point (3,7) at 2300 GMT, 10 June 1967. No vertical smoothing of the divergence field was applied.

Based on this, plus the fact that the divergence at any point must also be affected by the divergence at surrounding points, it was felt that a vertical smoothing should be performed and compared to Figure 7 in order to determine if a more realistic divergence pattern could be obtained.

Numerous vertical smoothing techniques were tried and discarded before a satisfactory one was finally obtained. The resultant vertical smoothing technique employed a three dimensional, space-centered, finite-difference smoothing scheme as depicted in Figure 8.

In the actual computation, a weighting factor was assigned to each point with the heaviest weight being given to the point being smoothed. Since the divergence field had already been smoothed in the horizontal, the next heaviest weight was equally given to the points immediately above and below the point to be smoothed. Finally, the horizontal points on each side were assigned the smallest weight. Various combinations of weights were tried to determine which combination would result in the most representative and realistic divergence patterns. The weighting factors finally chosen were those given in Figure 8.

The smoothing technique was modified at K=1 (950 mb) and K=17 (150 mb) as well as at the lateral borders since a space-centered smoothing scheme was not possible. This resulted in the elimination of one weighting factor of 3 at K=1 and K=17, and one weighting factor of 1 on each of the lateral boundaries. The results of this smoothing of the divergence field are shown in Figure 9 which depicts the same

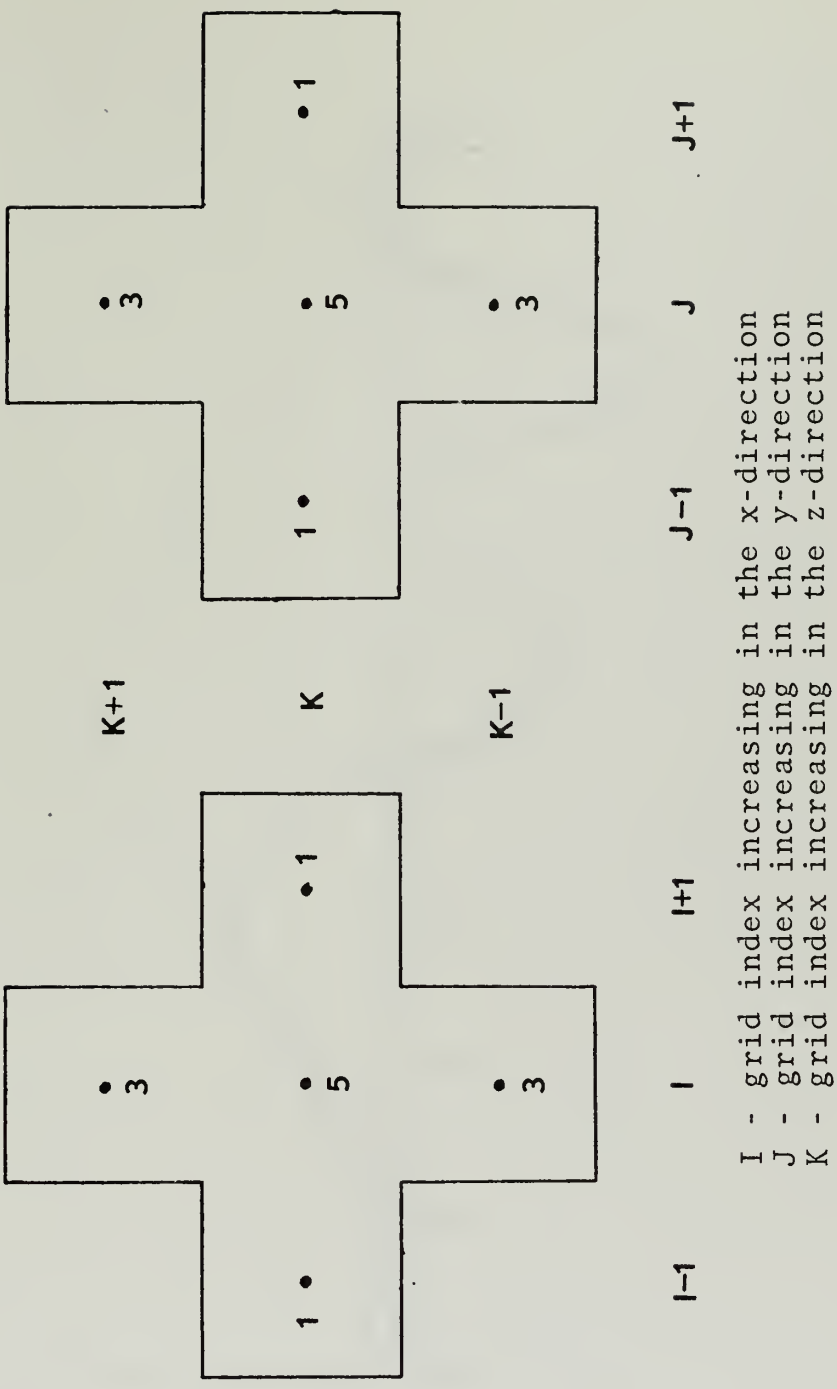

Fig. 8. Example of three-dimensional smoothing technique utilized in smoothing the divergence field in the vertical. Weighting factors assigned to each point are as indicated.

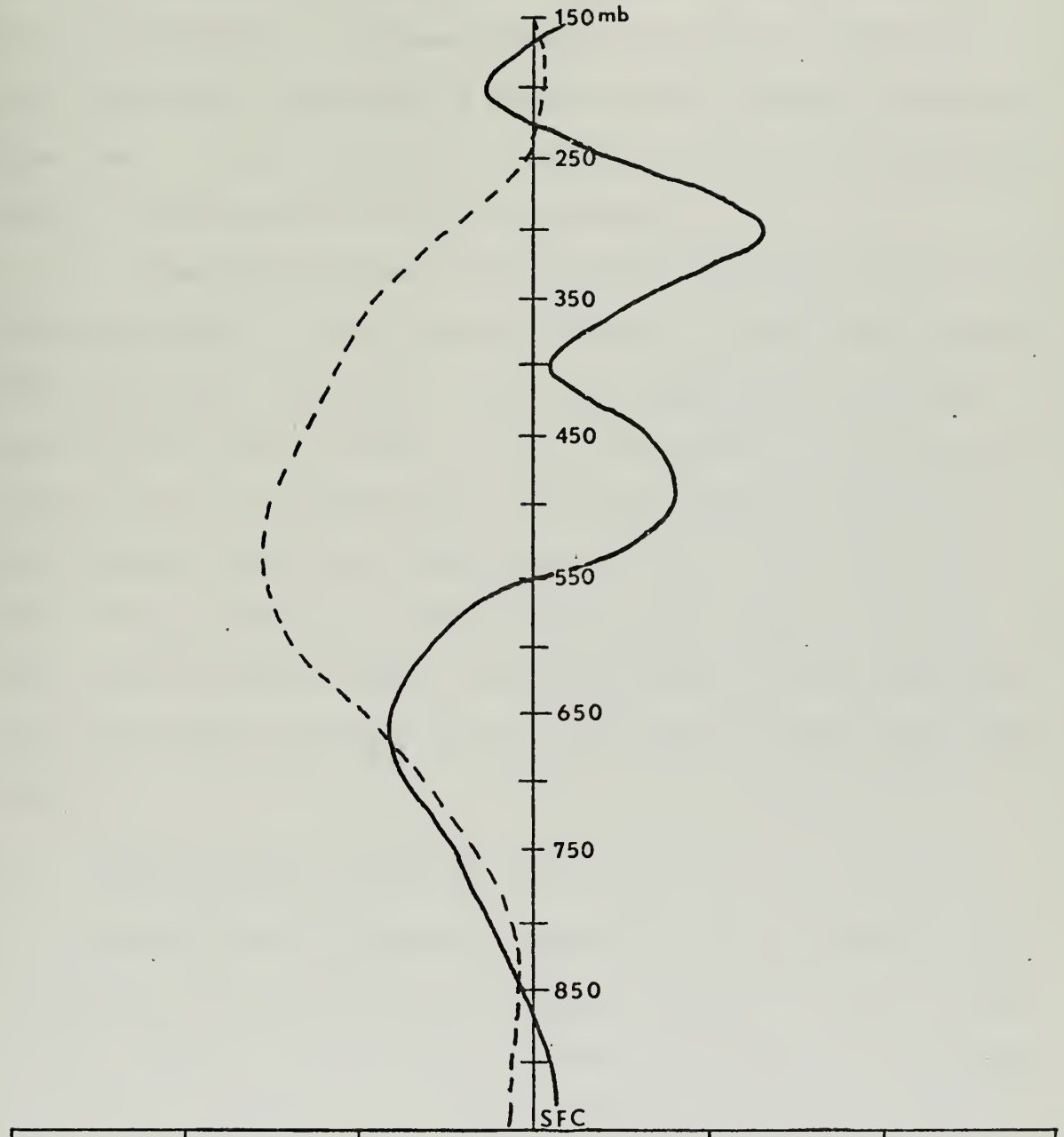

Fig. 9. Divergence and vertical motion for point (3,7) at 2300 GMT, 10 June 1967. Vertical smoothing of the divergence field was applied.

grid point as shown in Figure 7. Comparing these two figures, it was obvious that the extremes in the divergence field of Figure 7 had been damped in Figure 9, while the vertical motion patterns in both figures remained basically the same. It was therefore decided that the vertical smoothing of the divergence field was useful.

A final computation involving the divergence was to sum the divergence in each vertical column to see if the sum of the divergence was small. No values approached zero, but were of the order of 10^{-4} to 10^{-5} per second. If one used these values to compute the vertically averaged divergence, the results would be of the order of 10^{-5} to 10^{-6} per second. These values were deemed acceptable since an artificial lid, due to lack of data, had been placed on the atmosphere at 150 mb while convection may well have extended above this level.

C. VERTICAL MOTION COMPUTATIONS

Several vertical motion schemes have been developed for computing values of vertical motion (omega) on the synoptic scale. Whether or not these schemes would work on the mesoscale was the question. Since constant pressure surfaces were utilized in the analysis, this automatically eliminated computation of vertical motion by any of the isentropic methods. The thermodynamic methods were eliminated because of the difficulty in obtaining values for diabatic heating. The quasi-geostrophic form of the omega equation was not used because it required a Rossby number of less than 0.1, and on

the mesoscale it is not uncommon to obtain Rossby numbers greater than 2.0 in areas of strong convective activity.

After elimination of the above methods, only the kinematic and vorticity methods for computing vertical motions were left. The vorticity method, as discussed by Coleman (1969), was eliminated due to the result that computed values for vertical motion were not within the realm of acceptability on the mesoscale; that is, the values obtained became so large that they could no longer be believed.

Thus, by the process of elimination, the kinematic method of computing vertical motion was chosen. However, the kinematic method involves integration of the continuity equation:

$$\frac{\partial \omega}{\partial p} + \nabla \cdot \vec{V} = 0 \qquad (4)$$

which contains many disadvantages. These disadvantages may be categorized as follows:

1. Either an upper or lower boundary condition is required;
2. It is computed from divergences with the disadvantages discussed in the previous section;
3. It is very poor in regions of ill-defined winds; and
4. It tends to yield excessively large values, even in areas of good wind data.

Before the kinematic method could be used to compute the vertical motion it was necessary to provide solutions to the disadvantages listed above. An assumption of $\omega=0$ at 150 mb

was chosen in order to allow computation of a linear error term. This appeared to be an adequate assumption based on an inspection of the analyses which showed that the tropopause was located in the vicinity of 150 mb and at the tropopause vertical motion is generally assumed to approach zero. It was realized, however, that some vertical motion would probably penetrate the tropopause due to the strong convective activity that is known to be associated with severe thunderstorms. But since insufficient data (only two or three out of nine stations) was available above 150 mb to allow for a realistic analysis, this assumption was considered necessary.

The lower boundary condition of $\omega=0$ at the surface was not utilized because of the large amounts of convective activity and vertical motion that would normally be anticipated in an area of tornadoes and thunderstorms. Instead, the vertical motion at the surface was computed utilizing the terrain effects of the u and v components of the wind and the surface pressure, that is:

$$\omega_{sfc} = u \frac{\partial p}{\partial x} + v \frac{\partial p}{\partial y} = \vec{V} \cdot \nabla_h p_{sfc} \qquad (5)$$

where $\vec{V} \cdot \nabla_h p_{sfc}$ is expressed in cartesian coordinates.

The second and third disadvantages were minimized in this case due to the averaging techniques employed for the divergence in both the horizontal and vertical plus the fact that there were nine upper air reporting stations in the mesonetwork.

The last disadvantage presented the greatest degree of difficulty and the chief reason why most meteorologists have

not used the kinematic method in the past. Gruber and O'Brien (1968), and O'Brien (1970), have investigated this problem in great detail. O'Brien (1970) found that case studies for intense mesoscale convection demonstrated the reliability and usefulness of an adjustment scheme for the kinematic method which was based on the premise that the errors in the divergence field were a linear function of pressure.

Starting with the integrated form of the continuity equation:

$$\omega_u = \omega_L + \overbrace{\nabla \cdot \vec{V}}^{\sim\sim} (P_L - P_u) \tag{6}$$

where the integral average is approximated by $\overbrace{\nabla \cdot \vec{V}}^{\sim\sim}$, (the vertical average of the divergence field between two levels) the values of omega were successively computed, that is:

$$\omega_{900} = \omega_{sfc} + \left(\frac{DIV_{900} + DIV_{sfc}}{2} \right) (P_{sfc} - 900). \tag{7a}$$

Utilizing the value for omega at 900 mb to obtain the value of omega at 850 mb, yields:

$$\omega_{850} = \omega_{900} + \left(\frac{DIV_{850} + DIV_{900}}{2} \right) (50)$$

$$= \omega_{sfc} + \left(\frac{DIV_{900} + DIV_{sfc}}{2} \right) (P_{sfc} - 900)$$

$$+ 25 \left(DIV_{850} + DIV_{900} \right). \tag{7b}$$

Continuing this cumulative procedure through to 150 mb gives:

$$\omega_{150} = \omega_{sfc} + \left(\frac{DIV_{900} + DIV_{sfc}}{2} \right) (P_{sfc} - 900)$$

$$+ 25 \left(DIV_{900} + DIV_{150} + 2 \Sigma DIV_{(850 \rightarrow 200)} \right) \tag{7c}$$

where $\Sigma DIV_{(850\rightarrow200)}$ means the sum of all of the divergence terms between 850 mb and 200 mb. Now, it was assumed earlier that $\omega_{150}=0$, thus, equation (7c) may be rewritten as:

$$0 = \omega_{sfc} + \left\{\frac{DIV_{900} + DIV_{sfc}}{2}\right\}(P_{sfc} - 900)$$

$$+ 25\ (DIV_{900} + DIV_{150} + 2\Sigma DIV_{(850\rightarrow200)}). \qquad (7d)$$

Dividing equation (7d) by 25 mb in order to place the equation in units per second yields:

$$0 = \frac{\omega_{sfc}}{25} + \left\{\frac{DIV_{900} + DIV_{sfc}}{50}\right\}(P_{sfc} - 900)$$

$$+ DIV_{900} + DIV_{150} + 2\Sigma DIV_{(850\rightarrow200)}. \qquad (7e)$$

If ω_{150} actually was zero, if all divergence terms were exact, and if there was no computer round-off error, then equation (7e) would be identically satisfied. It is obvious that this is not the case and thus (7e) is only approximately satisfied. The difference between zero and the value obtained by the above relationship is the error term. Calling this divergence error term DVERT, and setting it equal to the previous relationship yields:

$$DVERT = \frac{\omega_{sfc}}{25} + \left\{\frac{DIV_{900} + DIV_{sfc}}{50}\right\}(P_{sfc} - 900)$$

$$+ DIV_{900} + DIV_{150} + 2\Sigma DIV_{(850\rightarrow200)}. \qquad (7f)$$

Now dividing DVERT by the sum of the multipliers of the divergence terms and the vertical motion at the surface, or equivalently, $(P_{sfc}-150)x0.04$, resulted in an average error

for the divergence throughout the vertical. This corresponded to O'Brien's (1970) statement that the errors in the divergence field were a linear function of pressure. Subtracting this error from the computed averaged divergence at each level resulted in a corrected divergence which was then used in the computation of the vertical motion. The results of utilizing this method can be seen from Figure 7 and Figure 9. In addition, the average values of omega at 150 mb in this study were 10^{-7} mb sec^{-1} or 8.6×10^{-3} mb day^{-1}, well within the acceptable tolerances established prior to beginning this study.

D. STATIC ENERGY COMPUTATIONS

Total energy may be defined as

$$E_T = C_p T + gZ + Lq + \frac{V^2}{2} \qquad (8)$$

where C_p is the specific heat of air at constant pressure, T the temperature, gZ the geopotential, L the latent heat, q the specific humidity, and V the scalar velocity. The substantial derivative of total energy is given by the relationship:

$$\frac{d}{dt}\left(C_p T + gZ + Lq + \frac{V^2}{2}\right) = \frac{dh}{dt} + \alpha \frac{\partial p}{\partial t} + F \qquad (9)$$

where dh/dt represents the sum of sensible heat, evaporation, and radiation, α is the specific volume, $\partial p/\partial t$ is the local pressure change, and F represents frictional heating. Now, assuming that the sum of the terms on the right of equation (9) are sufficiently small, one may write

$$\frac{d}{dt}\left(C_pT + gZ + Lq + \frac{V^2}{2}\right) \simeq 0 . \tag{10}$$

Since static energy is defined as

$$E_s = C_pT + gZ + Lq \tag{11}$$

equation (10) may be written

$$\frac{d}{dt} E_s + \frac{d}{dt}\left(\frac{V^2}{2}\right) \simeq 0. \tag{12}$$

Since $d/dt(V^2/2)$ is a relatively small term, as verified by utilizing observed winds, the static energy was assumed to be conservative.

The conservative nature of E_s may be further understood by writing

$$C_p \frac{T}{\theta_E} \frac{\partial \theta_E}{\partial p} \simeq \frac{\partial}{\partial p} (C_pT + gZ + Lq) \tag{13}$$

and recalling that θ_E is conserved for both dry- and saturated-adiabatic displacement. It follows that the difference in static energy between two levels is directly related to the potential instability of the layer.

In addition, the normal instrument tolerances in a radiosonde allow the additional assumption of $q \simeq w$, where w is the mixing ratio. Thus, the static energy may be expressed by the following approximate relation:

$$E_s \simeq C_pT + gZ + Lw. \tag{14}$$

The first item investigated was the total derivative of static energy. Utilzing a space- and time-centered finite differencing scheme, the total derivative of static energy was obtained using the expansion:

$$\frac{dE_s}{dt} = \frac{\partial E_s}{\partial t} + u\frac{\partial E_s}{\partial x} + v\frac{\partial E_s}{\partial y} + \omega\frac{\partial E_s}{\partial p} = \frac{\partial E_s}{\partial t} + \vec{V}\cdot\nabla E_s + \omega\frac{\partial E_s}{\partial p}. \quad (15)$$

The results obtained from computing the total derivative were of the order of 10^{-2} $m^2(s^2\text{-}1.5hr)^{-1}$. The total derivative of static energy was computed to check how well the finite differencing scheme employed conserved static energy.

Assuming $dE_s/dt=0$, the local rate of change of static energy was computed from the advective terms. The local rate of change of static energy can be expressed by:

$$\frac{\partial E_s}{\partial t} = -\left(u\frac{\partial E_s}{\partial x} + v\frac{\partial E_s}{\partial y} + \omega\frac{\partial E_s}{\partial p}\right) = -\left(\vec{V}\cdot\nabla E_s + \omega\frac{\partial E_s}{\partial p}\right). \quad (16)$$

The values obtained for the local rate of change of static energy using equation (16) were of the same order of magnitude as those values obtained for the total derivative of static energy. These values were then used as a prognostic tool by taking a single forward time step to obtain the static energy at time $t + \Delta t$, where Δt is 1.5 hours. This may be expressed in equation form by:

$$E_{t+\Delta t} = E_t + \left(\frac{\partial E}{\partial t}\right)\Delta t \quad (17)$$

No boundary conditions were required in computing $E_{t+\Delta t}$ as the forecast was confined to the interior grid points. It was realized that the prognostic values of $E_{t+\Delta t}$ would not exactly equal the actual values due to the assumptions previously made. However, it was desired to see if the prognostic values could be used to predict an accurate energy index based on the premise that the generated errors of the

prognostic static energy would cancel each other out in the computation of the energy index.

The Energy Index was defined by Darkow (1968) as

$$E.I. = (E_{T500} - E_{T850}) \tag{18}$$

with values in joules gm^{-1} indicating the following:

1. 0.0 to -4.2 -- thunderstorms possible;
2. -4.2 to -8.4 -- isolated severe thunderstorm activity possible; and
3. <-8.4 -- severe thunderstorms and associated tornado activity are highly probable.

The above criteria are conditional upon an adequate triggering mechanism being present or forecast to release the potential instability.

The prognostic Energy Indexes obtained by subtracting the forecast static energy at 850 mb from that forecast for 500 mb, were compared to the actual Energy Indexes to determine if they were in general agreement. Finally, the static energy computations were compared with the divergence and vertical motion patterns to determine if any correlation existed. Results of these comparisons are included in the following section.

IV. RESULTS

To facilitate the discussion of the results of this study, each time frame is looked at separately and in sequence beginning with 2300 GMT, 10 June 1967. All figures in this chapter are on a 12X10 grid, with parameters calculated on the 10X8 grid extrapolated one grid distance in each direction on the boundaries. This expansion of the reduced grid was necessitated by the fact that many of the tornadoes and thunderstorms occurred on the northern boundary of the 12X10 grid, and utilization of the 10X8 grid would result in these features being excluded.

The space-centered finite differencing schemes used throughout this study along with the original data and analysis problems resulted in the border areas being the areas where the greatest errors occurred. To prevent any bias from being introduced into the analysis, it was decided that the locations and times of the tornadoes and thunderstorms should not be known until all analysis and data extraction had been performed. As a result, the areas of greatest tornado and thunderstorm activity were also the areas where the greatest probability of errors existed.

The 750 mb level was used throughout this section to represent the divergence and vertical motion patterns for all time frames. This level was chosen because it was illustrative of the low level air involved in the convection.

All tornado and thunderstorm locations indicated on the figures in this chapter were obtained from either Storm Data

(1967) or zero degree elevation radar pictures taken by the WSR-57 radar located at Norman, Oklahoma.

A. THE MESOSCALE SITUATION AT 2300 GMT, 10 June 1967

Figure 10 shows the actual Energy Index for the first time frame. From the values shown in this figure, the entire mesonetwork was an area of probable tornado activity with all values more negative than -12, and with a relative maximum probability located in the northwest quadrant where a tornado did occur at 2309 GMT. A thunderstorm was also contained in the area of maximum probability.

Figure 11 shows the divergence and vertical motion patterns at 750 mb for the same time. The tornado and thunderstorm were seen to occur in an area of ascending vertical motion and strong horizontal convergence. In addition, there were relative maximums of both convergence and ascending vertical motion ahead of the tornado and thunderstorm. Behind these features, there were areas of divergence and descending vertical motions. Both of these results conformed to models previously developed for tornadoes and thunderstorms (cf. Browning and Ludlam, 1962). It may also be noted from Figure 11 that it was not possible to exactly locate the tornado based on the divergence and vertical motion patterns as a tornado is normally considered to be a sub-mesoscale phenomena.

B. THE MESOSCALE SITUATION FOR 0030 GMT, 11 June 1967

Figure 12 shows both the actual and the forecast Energy Indexes for 0030 GMT, 11 June 1967. The actual Energy Index

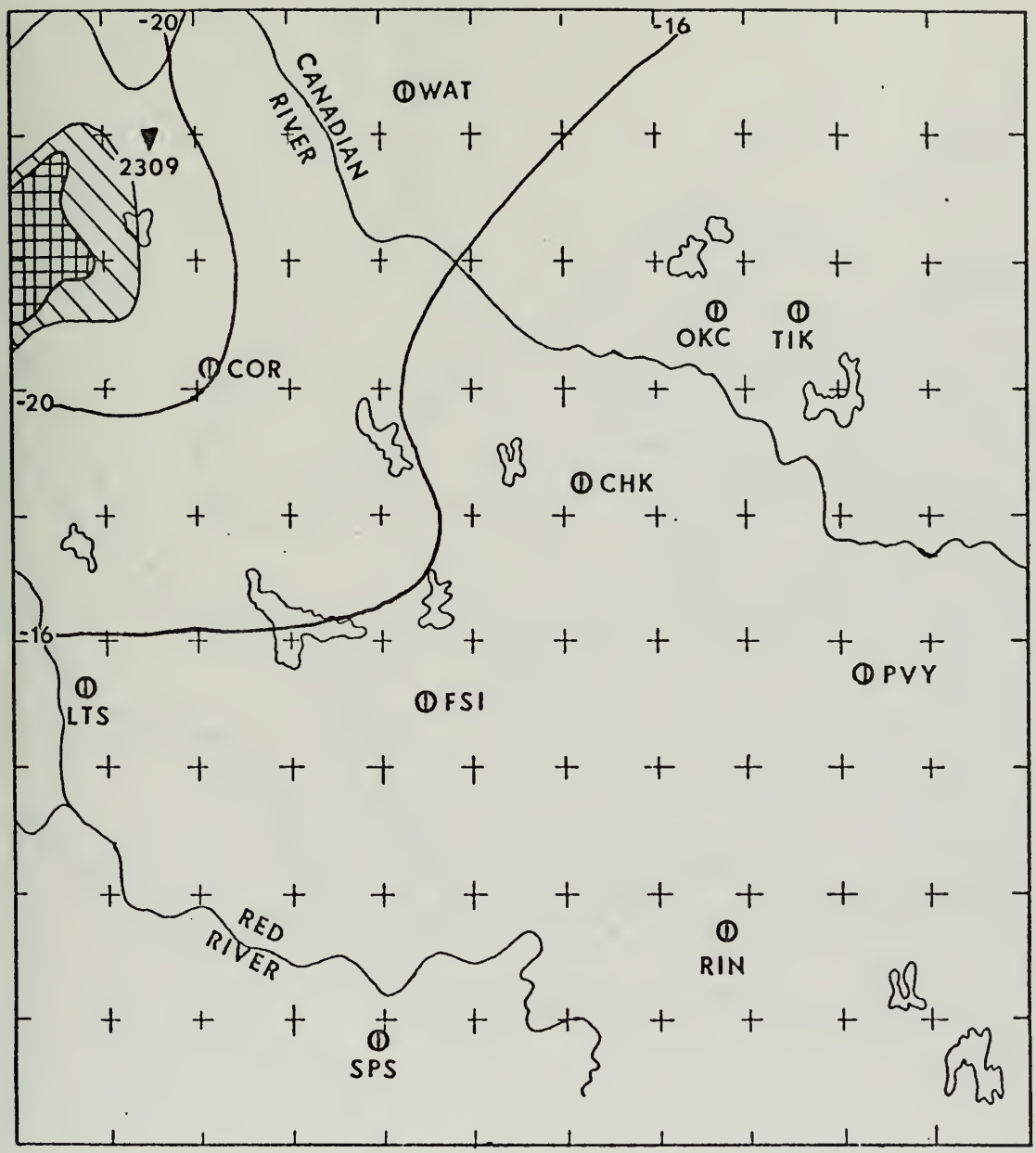

Fig. 10. Energy Index for 2300 GMT, 10 June 1967. All values are in joules gm^{-1}. ▼ indicates tornado activity, ⊕ indicates maximum radar return, and ⊗ indicates secondary radar return.

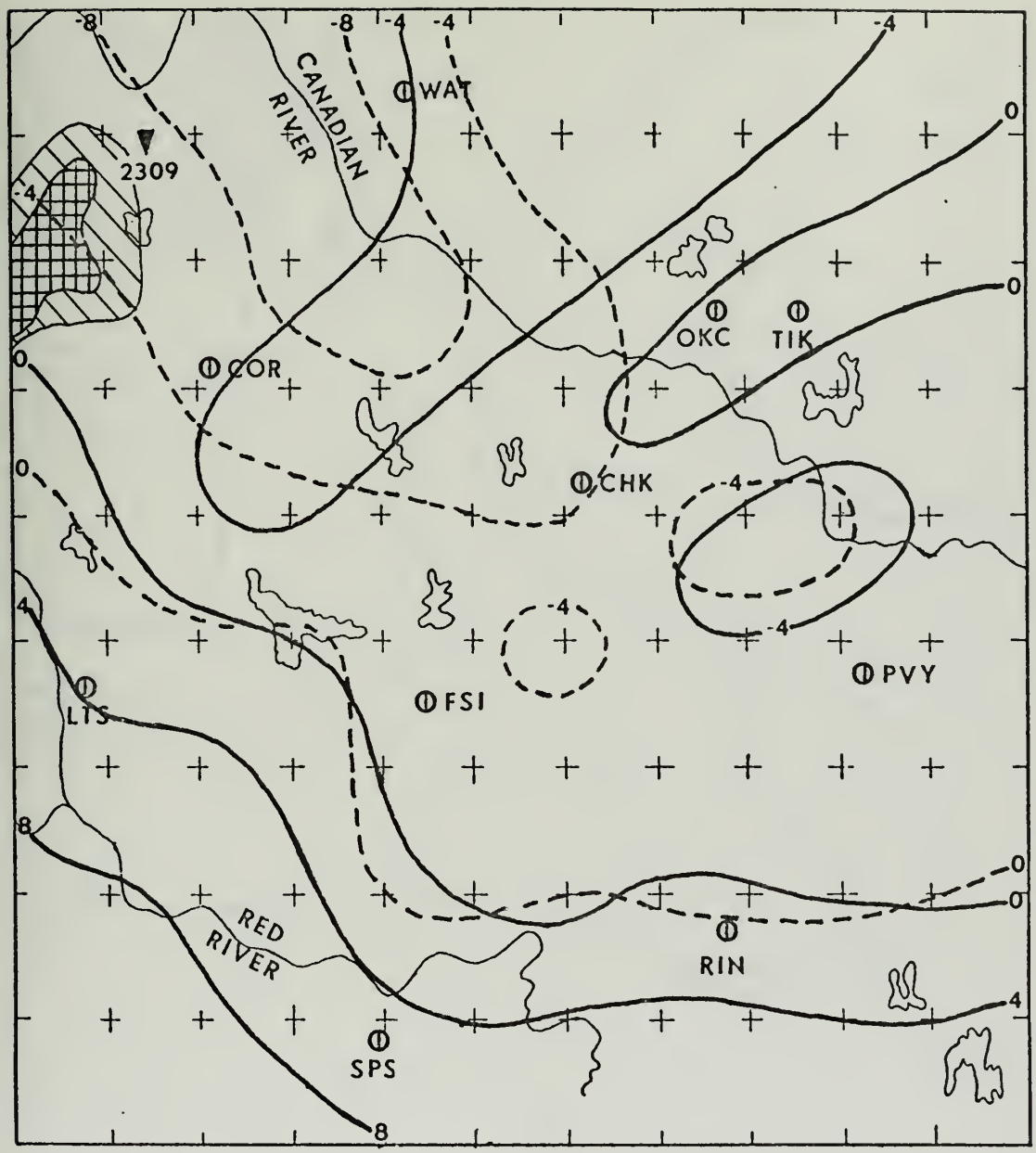

Fig. 11. Divergence (---)x10^{-5} sec^{-1} and vertical motion (——)x10^{-3} mb sec^{-1} at 750 mb for 2300 GMT, 10 June 1967. ▼ indicates tornado activity, ⊕ indicates maximum radar return, and ⊕ indicates secondary radar return.

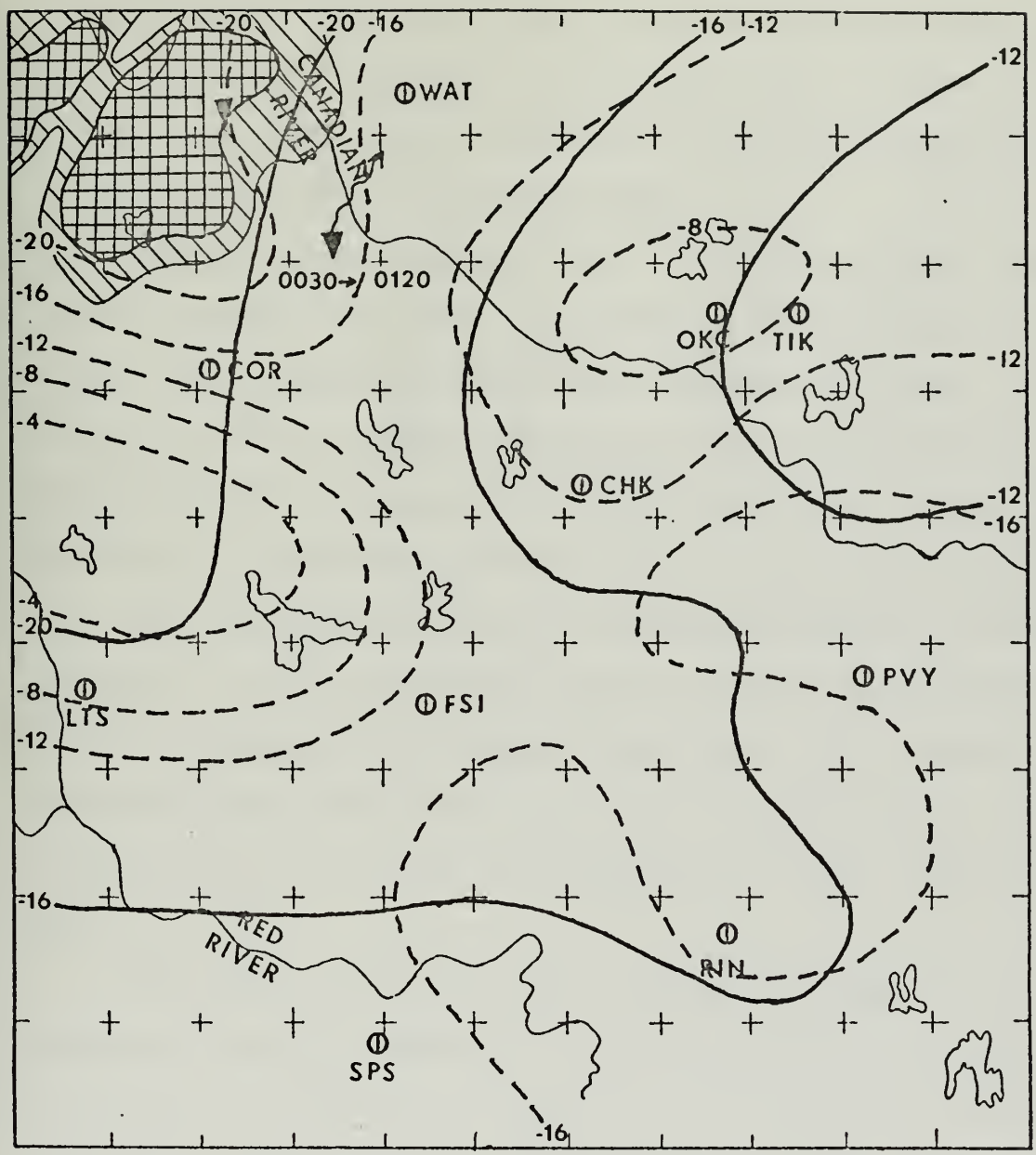

Fig. 12. Actual (——) and forecast (---) Energy Indexes for 0030 GMT, 11 June 1967.

indicated once again that the entire mesonetwork was a probable tornado and thunderstorm activity area. There was a relative maximum area of probability in the northwest and a relative minimum in the northeast.

The prognostic Energy Index also indicated that the entire mesonetwork, with the exception of the western section, was a probable tornado and thunderstorm area. An area of relative maximum probability was located in the northwest with the area of minimum probability situated in the west. A secondary minimum was located in the northeast.

The two areas of relative maximum probability compared favorably as did the actual Energy Index minimum with the forecast Energy Index secondary minimum. The tornadoes and thunderstorms both occurred in the relative maximum areas of probability, that is, in areas smaller than -16 joules gm^{-1}.

There was generally good correlation between the two indexes, although the western area of the forecast Energy Index was an exception. Figure 13, the divergence and vertical motion patterns for the same time period, showed that the area of minimum probability in the forecast Energy Index corresponded to an area of strong descending vertical motion and divergence. The secondary area of minimum probability in the forecast Energy Index also corresponded to an area of divergence and weak descending vertical motion.

Both Energy Indexes correlated well with the vertical motion patterns in the vicinity of the tornadoes and thunderstorms. However, there appeared to be a stronger relationship

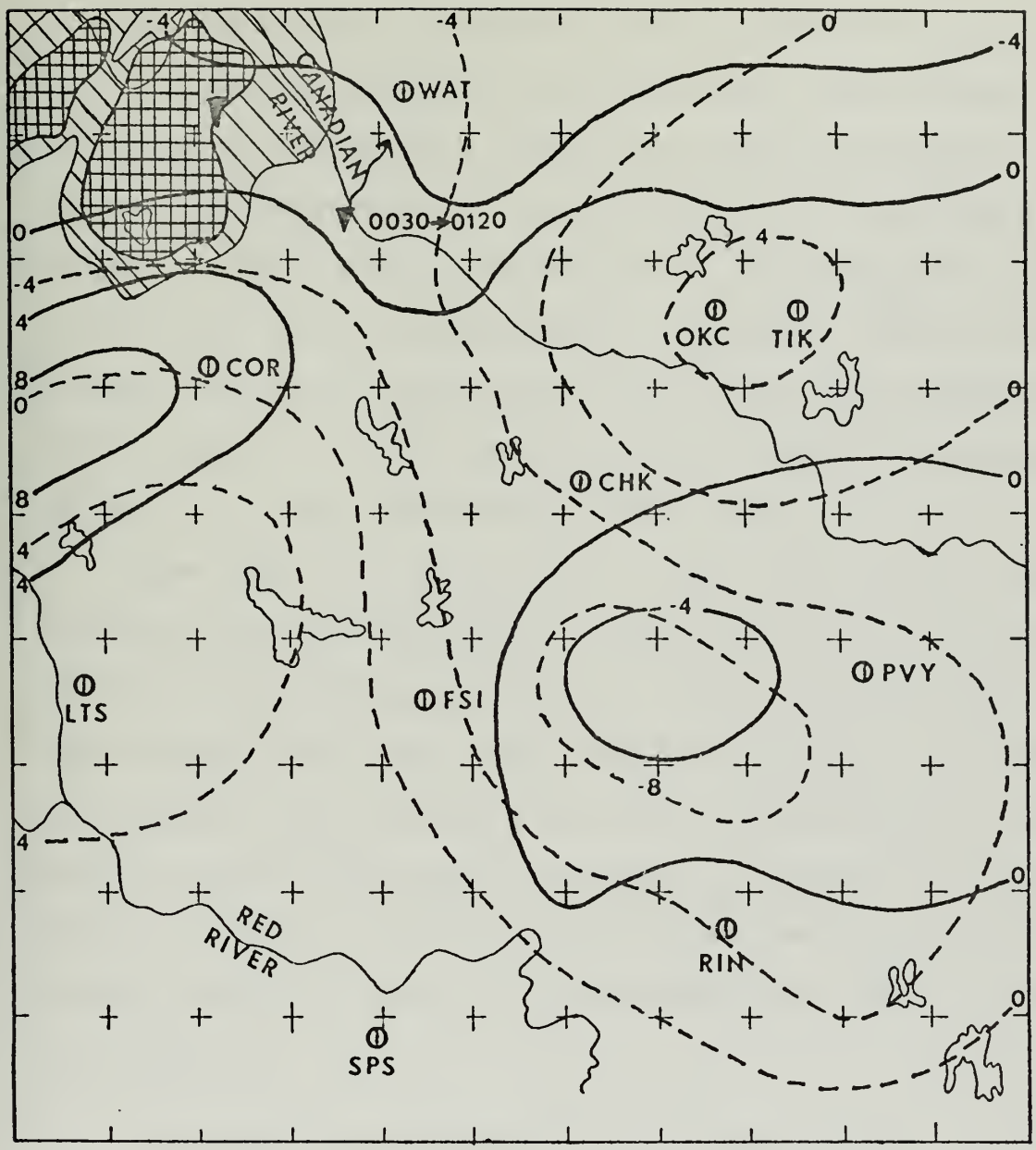

Fig. 13. Divergence (---)x10^{-5} sec^{-1} and vertical motion (——)x10^{-3} mb sec^{-1} at 750 mb for 0030 GMT, 11 June 1967.

between the prognostic Energy Index and the divergence and vertical motion patterns than between the actual Energy Index and the divergence and vertical motion patterns. This was not considered unusual when the method of obtaining the prognostic Energy Index was reviewed. The prognostic Energy Index for $t+\Delta t$ was obtained by adding the static energy at time t to the local rate of change of static energy at time t; and the local rate of change was heavily dependent on the u, v, and ω components of the wind.

From Figure 13 it can be seen that the tornadoes and thunderstorms once again were located in areas of ascending vertical motion and convergence. Ahead of the tornadoes and thunderstorms there was ascending vertical motion and convergence, while behind them there was descending vertical motion and weak convergence changing to divergence. Once again, it was not possible to determine the exact location of the tornadoes based on the divergence and vertical motion patterns.

C. THE MESOSCALE SITUATION FOR 0200 GMT, 11 June 1967

The observed Energy Index and the forecast Energy Index for 0200 GMT, 11 June 1967, are contained in Figure 14. The observed Energy Index indicated that the whole mesonetwork area was a probable tornado and thunderstorm area. A relative maximum area of probability was located in the northwest sector with a relative minimum area of probability located in the northeast section. The tornadoes and the thunderstorms actually occurred in the north, between the two extremes.

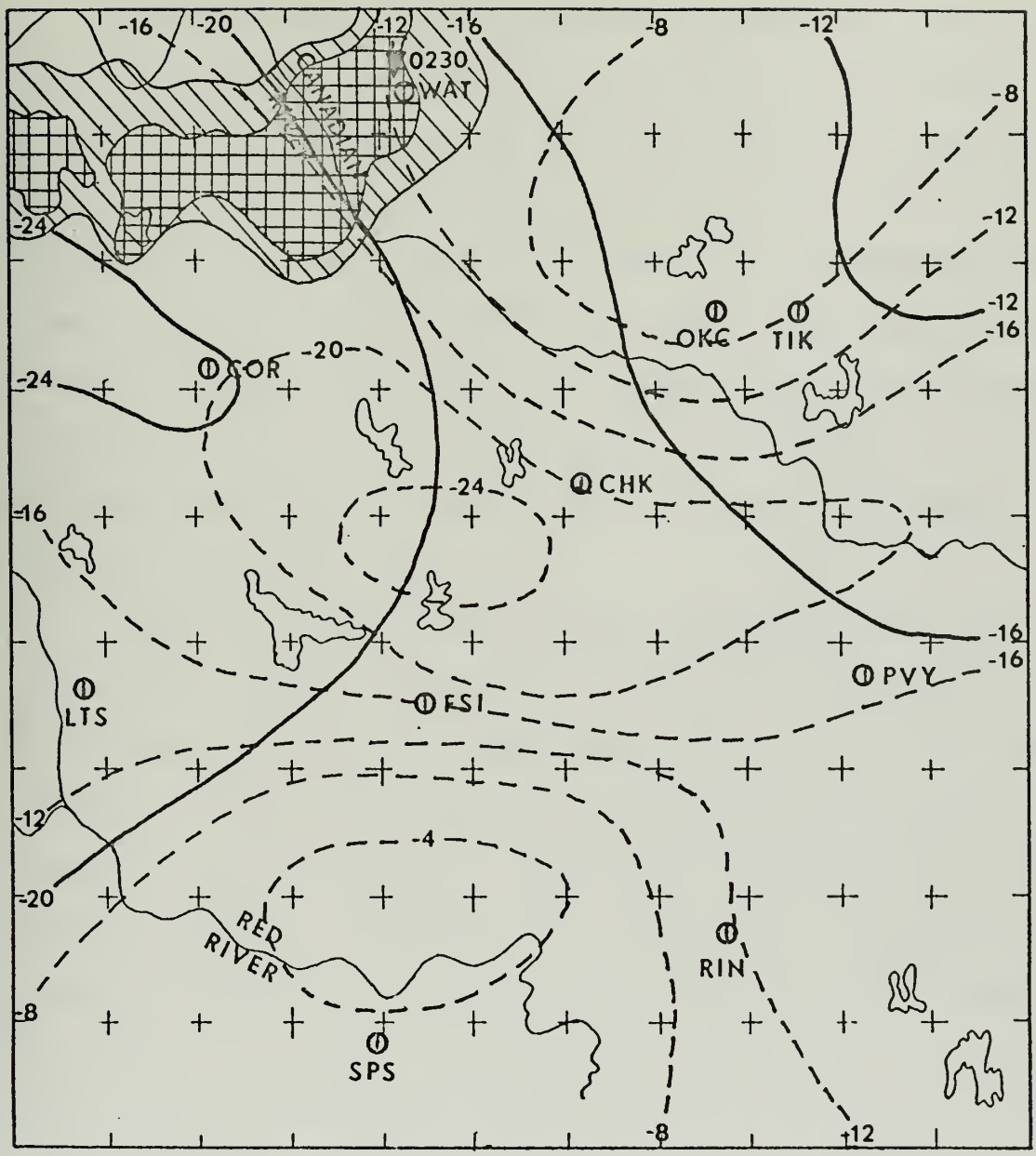

Fig. 14. Actual (——) and forecast (---) Energy Indexes for 0200 GMT, 11 June 1967.

The prognostic Energy Index also indicated that the entire mesonetwork was a probable area of tornado and thunderstorm activity, with the exception of the southern area. The forecast Energy Index indicated a relative maximum area of probability in the center of the network with two areas of minimum probability, one in the southern section of the grid and the other located in the northeastern section. As in the case with the actual Energy Index, the tornado and thunderstorms occurred in a highly probable tornado and thunderstorm area.

Figure 15 shows the divergence and vertical motion patterns for the same time frame. The tornado and thunderstorms occurred in an area of ascending vertical motion and convergence. Strong ascending vertical motion and convergence were ahead of them, although a pocket of divergence and descending vertical motion appeared to be in the area. The word "appeared" was chosen because it was not known what actually existed in the area as Watonga did not launch a radiosonde. Thus, all data north of Cordell and Tinker had to be extrapolated both in time and space as previously discussed. This is obviously an unsatisfactory procedure in dealing with a mesoscale investigation of tornadoes and thunderstorms.

D. THE MESOSCALE SITUATION FOR 0330 GMT, 11 June 1967

Figure 16 outlines the actual and forecast Energy Indexes for the fourth time frame. The actual Energy Index indicated that the entire mesonetwork was a probable tornado and thunderstorm activity area, with a relative minimum of

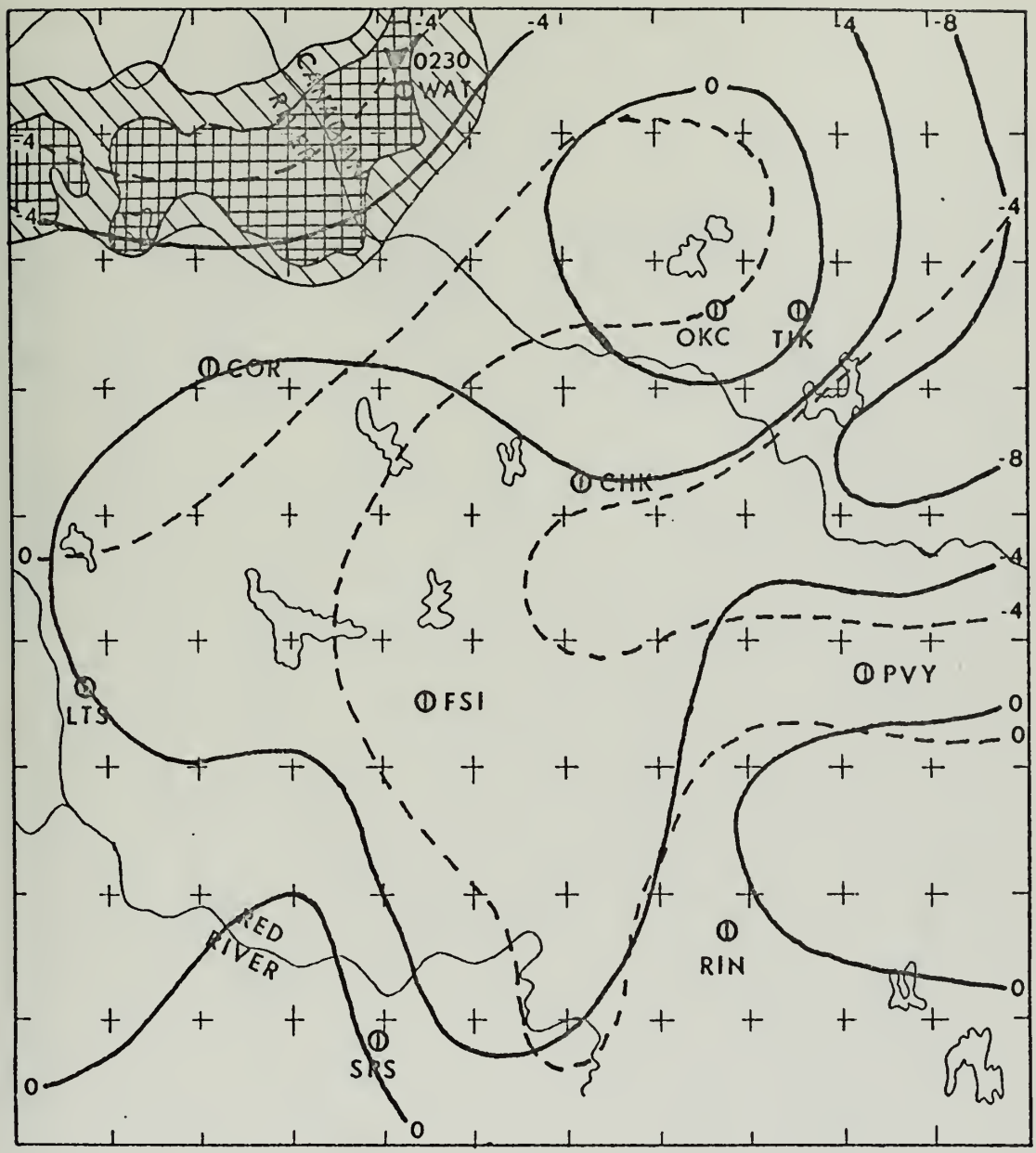

Fig. 15. Divergence (---)$x10^{-5}$ sec^{-1} and vertical motion (——)$x10^{-3}$ mb sec^{-1} at 750 mb for 0200 GMT, 11 June 1967.

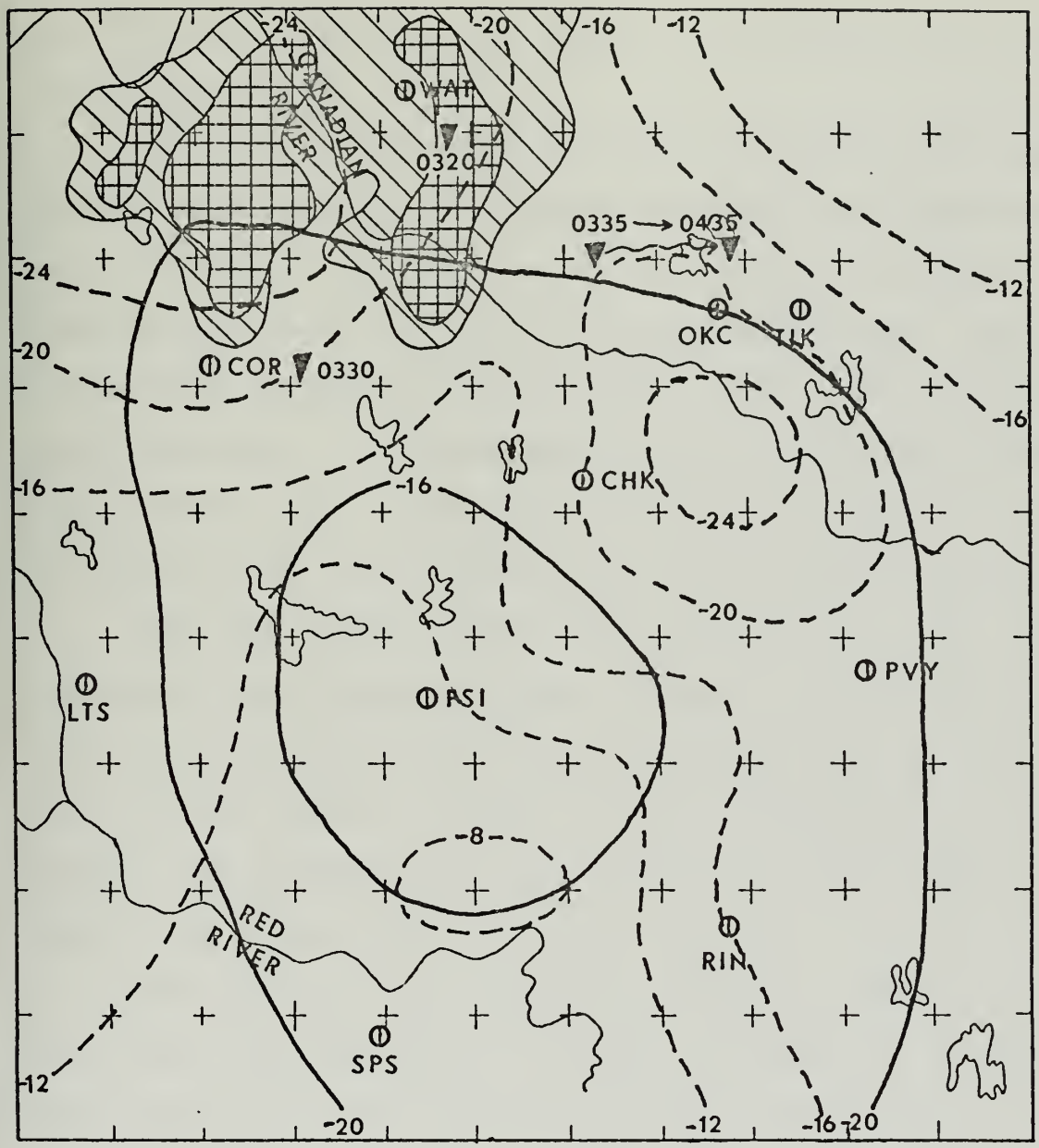

Fig. 16. Actual (——) and forecast (---) Energy Indexes for 0330 GMT, 11 June 1967.

probability located in the center of the network and increasing outward.

The prognostic Energy Index also indicated that the entire mesonetwork was a probable tornado and thunderstorm activity area. There was a relative minimum located in the same general area as for the actual Energy Index. Two areas of maximum probability also existed; one in the northwest and the other in the east-central section of the network. The tornadoes and thunderstorms occurred in areas of maximum probability for both forecast and actual Energy Indexes.

The correlation between the actual Energy Index and the forecast Energy Index was poor. However, there was a stronger relationship between the forecast Energy Index and the vertical motion pattern, Figure 17, in the vicinity of the tornadoes and thunderstorms than between the actual Energy Index and the vertical motion patterns.

The tornadoes all occurred in areas of ascending vertical motion and low-level horizontal convergence, with the same features located ahead of them in their projected path of movement. Some portions of the thunderstorms, however, occurred in areas of descending vertical motion and strong horizontal convergence; an apparent contradiction.

Re-analysis of the streamline and isotach patterns for this time period failed to improve the vertical motion patterns at low levels. The probable cause for this failure was the fact that both Watonga (WAT) and Tinker (TIK) failed to launch radiosondes, Watonga for the second successive time.

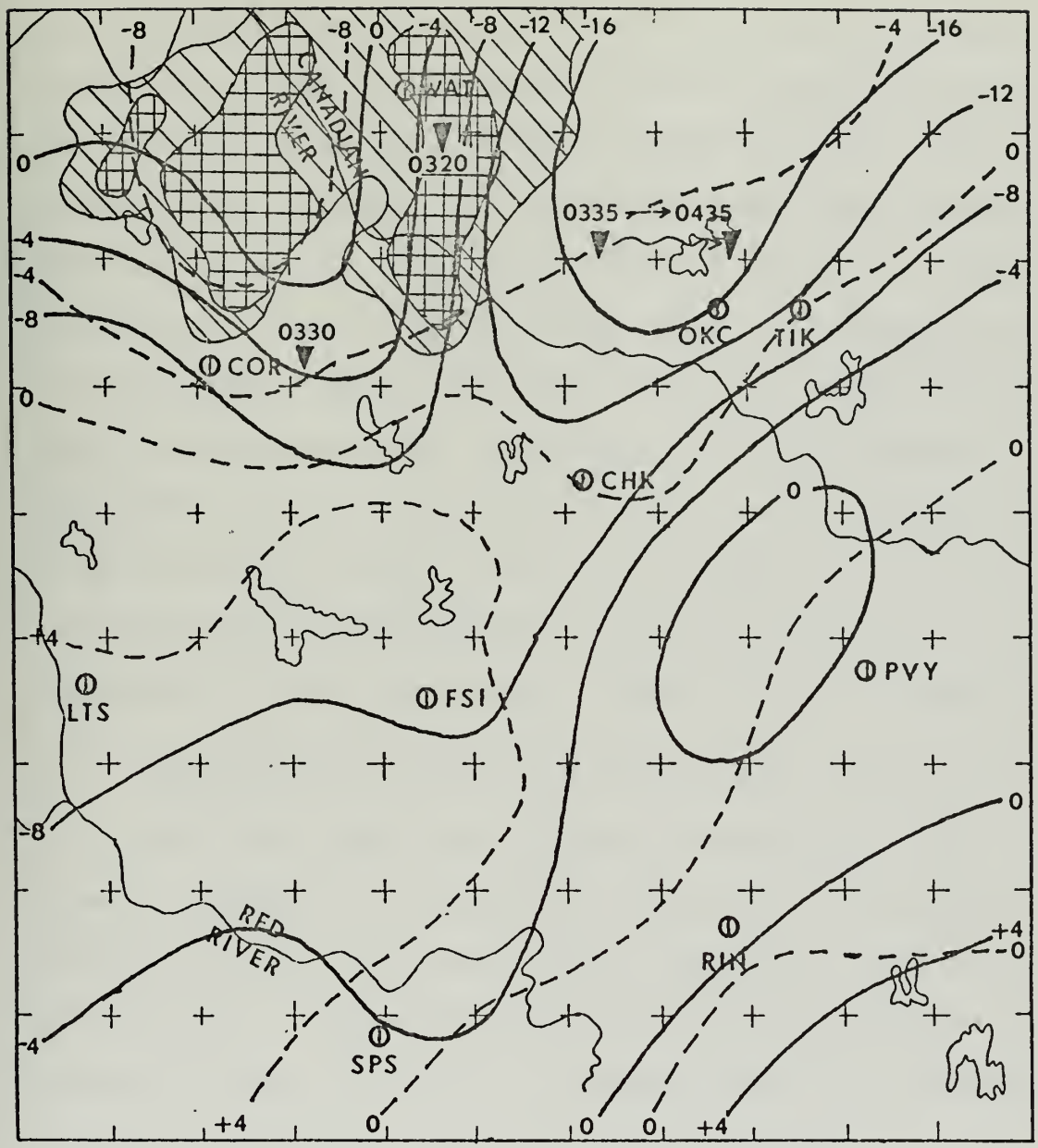

Fig. 17. Divergence (---)$x10^{-5}$ sec^{-1} and vertical motion (——)$x10^{-3}$ mb sec^{-1} at 750 mb for 0330 GMT, 11 June 1967.

As a result, it was necessary to extrapolate the entire northern section of the network for two time frames as well as extrapolate in space from the southern and central sections of the network. A single time frame extrapolation at 0200 GMT resulted in an area of probable error as previously discussed. Thus, with the large amount of convective activity present during this time frame as evidenced by the many thunderstorms and tornadoes, it was not possible to adequately portray the actual divergence and vertical motion patterns present. All of this points out the fact that any numerical investigation of mesoscale phenomena is severely hampered when space and time extrapolations are required.

E. THE MESOSCALE SITUATION FOR 0500 GMT, 11 June 1967

The actual and forecast Energy Indexes for the last time frame investigated are shown in Figure 18. Once again, the actual Energy Index showed the entire mesonetwork as a probable tornado and thunderstorm activity area with the northwestern section as a relative maximum area of probability and the northeastern area a relative minimum.

The prognostic Energy Index contained a maximum area of probability in the western section of the grid and an area of relative minimum probability in the north-central section. Both the actual and forecast Energy Indexes had the tornadoes and thunderstorms occurring in areas of probable activity.

A close look at the divergence and vertical motion fields, Figure 19, showed many apparent inconsistencies, such as strong ascending vertical motion occurring along with

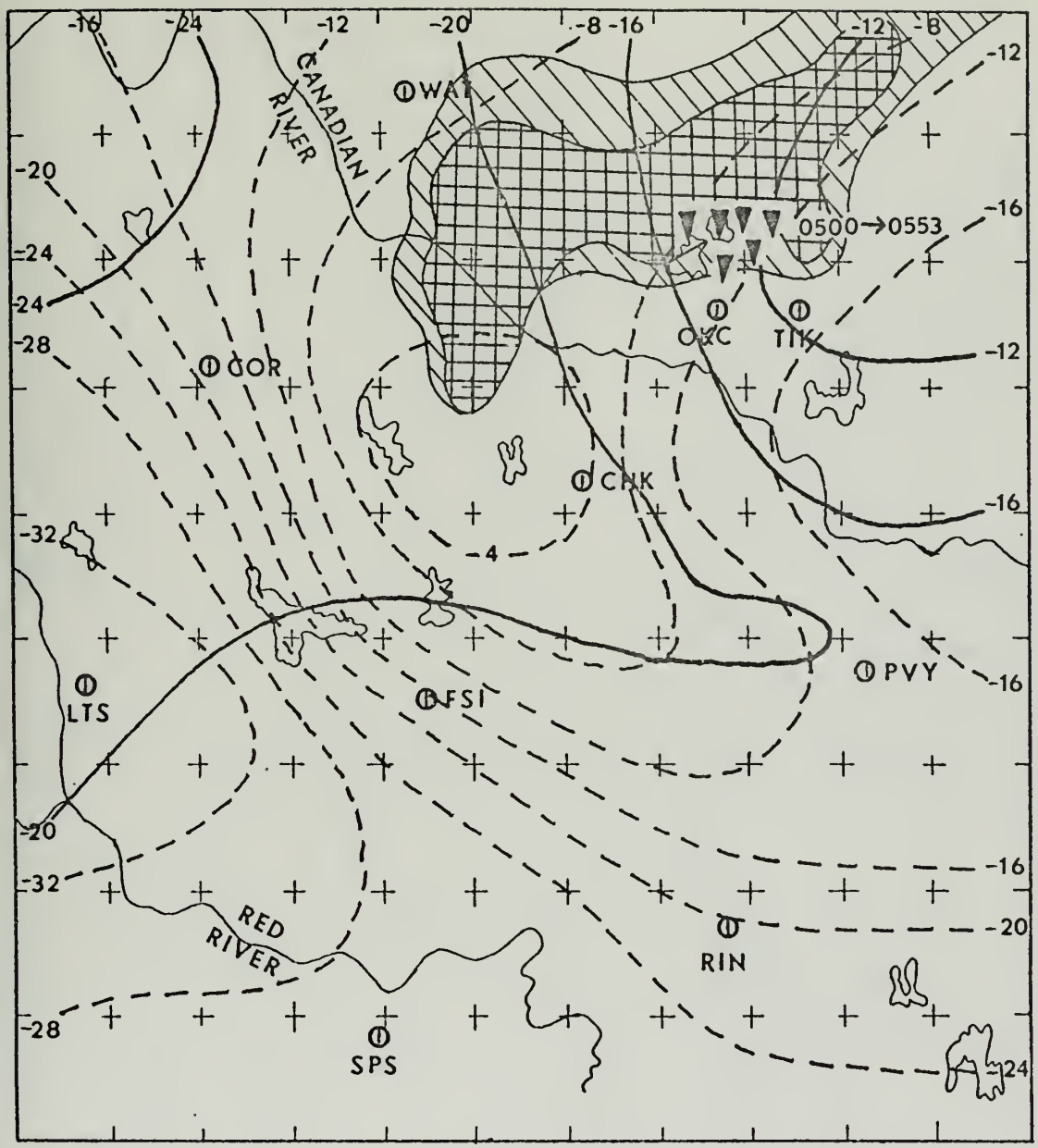

Fig. 18. Actual (——) and forecast (---) Energy Indexes for 0500 GMT, 11 June 1967.

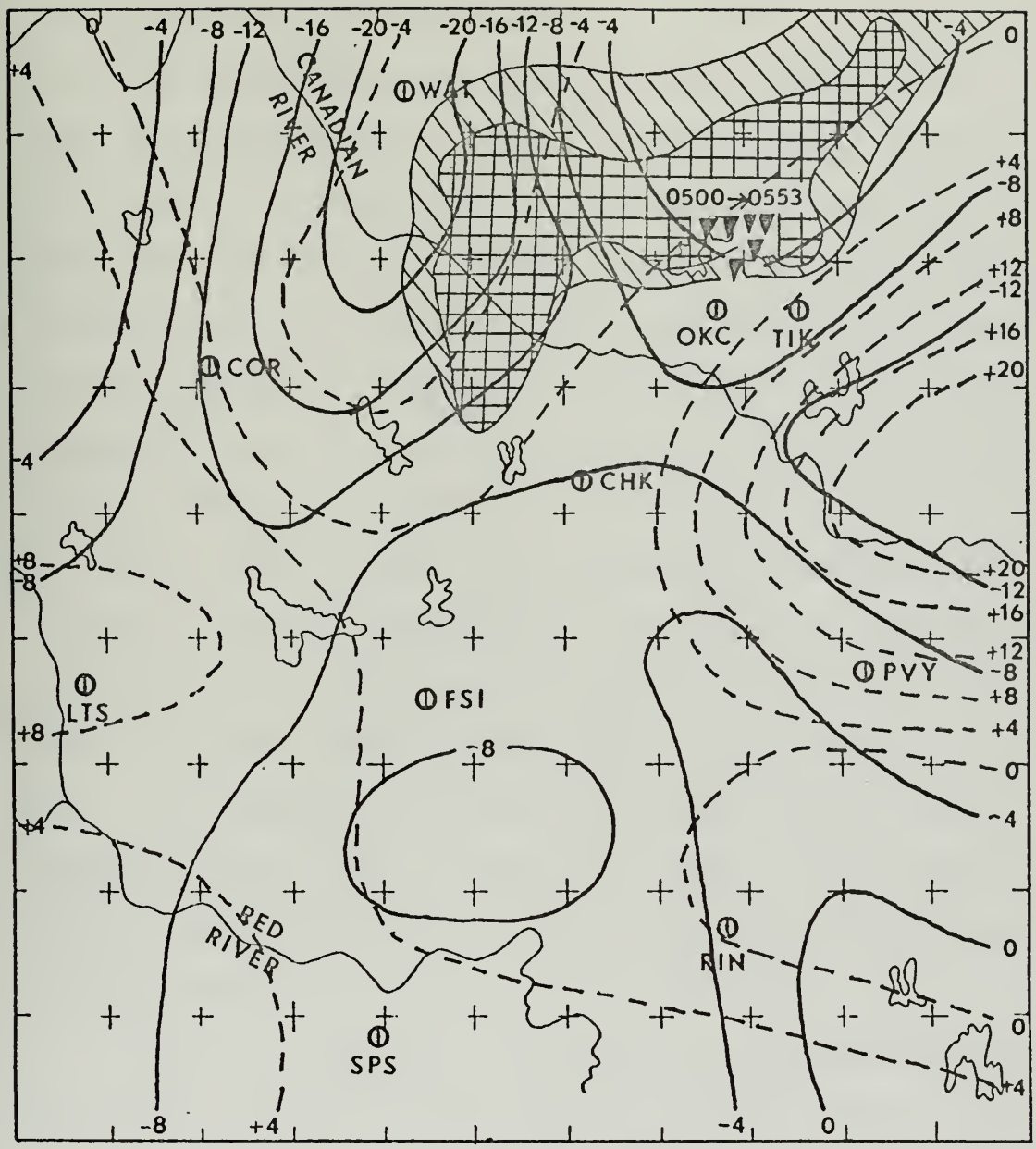

Fig. 19. Divergence (---)x10^{-5} sec^{-1} and vertical motion (——)x10^{-3} mb sec^{-1} at 750 mb for 0500 GMT, 11 June 1967.

strong horizontal divergence in the eastern section of the grid. Although this may appear to be a contradiction, it must be remembered that only the 750 mb level is illustrated. For this case, there was very strong horizontal convergence from the surface up to 800 mb, where it changed to horizontal divergence. The values of the ascending vertical motion had already started to decrease by 750 mb and finally became descending vertical motion by 650 mb. Thus, no inconsistencies actually existed.

As in the previous two time periods, Watonga (WAT) failed to launch a radiosonde. In addition, Tinker's (TIK) radiosonde data ended at 500 mb and the data was so different from the data at other stations as to be highly suspect. Once again, the entire northern section analysis depended upon a time extrapolation (this time covering three time periods) along with a space extrapolation from stations to the south.

This was obviously an unsatisfactory method of determining the divergence and vertical motion patterns, not only for this time frame, but for the previous two time frames as well. However, with no data available in the northern section of the grid during the last three times, the choice was either perform extrapolations or not use the last three time periods at all. Thus, although the results for these last three time periods may be poor compared to what actually occurred, they are still far superior to no results at all.

V. SUMMARY, CONCLUSIONS AND RECOMMENDATIONS

A. SUMMARY

On 10 June 1967, a series of tornadoes and thunderstorms passed through the NSSL mesoscale network in south-central Oklahoma, causing wide-spread damage and destruction. Utilizing the data provided by NSSL, this study investigated the divergence, vertical motion, and static energy relationships that existed in the NSSL network on that date during a five hour period from 2300 to 0500 GMT.

Divergence was computed using a trapezoidal, area-averaged, smoothing technique based on Gauss' Theorem. Investigation revealed that vertical smoothing of the divergence field was also desirable in keeping with Fankhauser's (1969) hypothesis that for mesoscale data, some form of smoothing is necessary. A five-point weighted smoother was utilized to compute the divergence field.

From the assumption that vertical motion at 150 mb was zero, a correction term was obtained that was linearly subtracted from the divergence field at each point in accordance with O'Brien's (1970) hypothesis that the errors in the divergence field are a linear function of pressure. Utilizing the corrected divergence field, vertical motion was computed by means of the kinematic method. The resulting computed vertical motion field was well constrained.

Investigation of the energy field centered about static energy. Operating on the principle of conservation of energy,

the total derivative of static energy was computed using a space and time centered finite difference scheme. This was done as a check on the data and the computational scheme.

Assuming that the total derivative of static energy was zero, the local rate of change of static energy was computed by setting it equal to the negative of the advective terms. Static energy fields were then forecast using the advective changes and a forward time step. The forecast static energy was then used to compute a prognostic Energy Index by subtracting the values at 850 mb from the values at 500 mb.

The prognostic Energy Index was compared to the actual Energy Index to determine if a correlation existed between the two indexes and between the indexes and the location of the tornadoes and thunderstorms. Finally, the divergence and vertical motion fields were compared to the location of the tornadoes and thunderstorms and to the Energy Indexes for possible correlation.

B. CONCLUSIONS

Based upon the results contained in Section IV, the following principle conclusions were made:

1. The computational method developed to smooth the divergence field resulted in a more realistic divergence pattern.
2. The corrected divergence constrained the kinematic method used in computing vertical motion and resulted in realistic vertical motion fields.

3. Lack of data in the northern section of the meso-network during the last three time frames resulted in rather poor divergence, vertical motion, and Energy Index patterns for those times.
4. The u and v components of the wind and the static energy fields should be smoothed prior to computing the total derivative and the local rate of change of static energy.

C. RECOMMENDATIONS FOR FUTURE RESEARCH

In line with the results and conclusions obtained in this study, the following recommendations were made concerning further research in the NSSL mesoscale network:

1. That a numerical program be developed to smooth the u and v components of the wind in such a manner that the divergence obtained by using smoothed values of u and v is the same as the divergence computed using Gauss' Theorem.
2. That a comparison of divergence and vertical motion fields be made utilizing the method contained in this study to the method suggested by Fankhauser.
3. That further research be conducted into utilizing static energy as a prognostic tool to localize the area of future probable tornado activity.
4. That a numerical program be developed specifically for the NSSL mesoscale network that would analyze data for all desired parameters in order to remove the subjective error from the analysis. In addition,

it could supplement the objective analysis techniques developed by NSSL which deal mainly with the 500 mb region as described by Inman (1970).

These are but four of many possible recommendations for future research in the field of mesometeorology. There are still many questions to be answered.

```
C     ************************************************************************
C     ************************************************************************
C     **                                                                    **
C     ** THIS COMPUTER PROGRAM, UNDER THE DIRECTION OF MY THESIS           **
C     ** ADVISOR, PROFESSOR RONNIE L. ALBERTY, IS SUBMITTED IN             **
C     ** PARTIAL FULFILLMENT FOR THE DEGREE OF MASTER OF SCIENCE           **
C     ** IN METEOROLOGY.                                                   **
C     ** THIS PROGRAM IS USED TO ASSIST IN THE MESOSCALE ANALYSIS          **
C     ** OF TORNADOES AND THUNDERSTORMS IN THE NATIONAL SEVERE             **
C     ** STORMS LABORATORY MESOSCALE NETWORK LOCATED AROUND OKLAHOMA       **
C     ** CITY, OKLAHOMA ON 10 JUNE 1967.                                   **
C     ** THIS PROGRAM USES AS INPUTS THE ANALYZED STREAMLINE, ISOTACH,     **
C     ** STATIC ENERGY, AND SURFACE PRESSURE FIELDS FOR FIVE TIME          **
C     ** PERIODS 90 MINUTES APART IN ORDER TO INVESTIGATE THE              **
C     ** DIVERGENCE AND VERTICAL MOTION FIELDS AND THE CONSERVATION        **
C     ** OF STATIC ENERGY.                                                 **
C     **                                LCDR LEO H. CRAIGLOW,JR., USN      **
C     **                                                                   **
C     ************************************************************************
C     ************************************************************************
C
C
C     THE PURPOSE OF THIS MAIN PROGRAM IS TO ESTABLISH THE CONSTANTS AND
C     LIMITS TO BE USED IN THIS THESIS AND TO CALL THE SUBROUTINES
C     THAT MAKE UP THE ENTIRE PROGRAM
C
      COMMON DD(12,10,17,5),VV(12,10,17,5),U(12,10,17,5),V(12,10,17,5),
     1DIV(12,10,17,5),W(12,10,17,5),P(17),PSFC(12,10,5),DX(10),
     2Q(12,10,5),DIVZER(12,10,5),ENG(12,10,17,5),DIVBAR(10,8),
     3WBAR(10,8),ENGBAR(10,8),II,JJ,KK,LL,DY,DT,ILESS,JLESS,KLESS,LLESS,
     4IIESS,JJESS,BL,BLI,PSI,EE(12,10,17,5)
C
C     THE FOLLOWING LIMITS AND CONSTANTS ARE TO BE USED THROUGHOUT THIS
C     PROGRAM:
C
C     II=THE NUMBER OF GRID POINTS IN THE X-DIRECTION
C     JJ=THE NUMBER OF GRID POINTS IN THE Y-DIRECTION
C     KK=THE NUMBER OF VERTICAL LEVELS UTILIZED IN THIS PROGRAM
C     LL=THE NUMBER OF TIME STEPS
C     DY=DISTANCE BETWEEN GRID POINTS IN THE Y-DIRECTION
C     DX=DISTANCE BETWEEN GRID POINTS IN THE X-DIRECTION
C     DT=TIME INCREMENT BETWEEN TIME STEPS IN SECONDS
C     BL=BASE LATITUDE OF GRID
C     BLI=BASE LATITUDE INCREMENT
```

```
C     THE VALUES ASSIGNED TO THE ABOVE LIMITS AND CONSTANTS ARE:
C
      II=12
      JJ=10
      KK=17
      LL=5
      ILESS=II-1
      JLESS=JJ-1
      KLESS=KK-1
      LLESS=LL-1
      IIESS=II-2
      JJESS=JJ-2
      DY=15.0
      DT=5400.0
      BL=33.75
      BLI=0.25
CCCCC
CCCCC CALL THE SUBROUTINES TO BE USED IN THIS PROGRAM
CCCCC
      CALL RREAD
      CALL CONST
      CALL DDOTV
      CALL OMEGA
      CALL ENERGY
      CALL PRNT1
      CALL ADVCT
      CALL PROG
C
      STOP
      END

      SUBROUTINE RREAD
CCCCCC
CCCCCC THE PURPOSE OF THIS SUBROUTINE IS TO READ IN VALUES OF WIND SPEED
CCCCCC (VV), WIND DIRECTION (DD), SURFACE PRESSURE (PSFC), STATIC ENERGY
CCCCCC (EE), AND TO COMPUTE THE PRESSURE LEVELS IN THE VERTICAL (P).
CCCCC
      COMMON DD(12,10,17,5),VV(12,10,17,5),U(12,10,17,5),V(12,10,17,5),
     1DIV(12,10,17,5),W(12,10,17,5),P(17),PSFC(12,10,5),DX(10),
     2Q(12,10,5),DIVZER(12,10,5),ENG(12,10,17,5),DIVBAR(10,8),
     3WBAR(10,8),ENGBAR(10,8),II,JJ,KK,LL,DY,DT,ILESS,JLESS,KLESS,LLESS,
     4IIESS,JJESS,BL,BLI,PSI,EE(12,10,17,5)
```

```
C      READ IN WIND DIRECTION, WIND SPEED, AND STATIC ENERGY FOR 17
CC     LEVELS AND 5 TIME STEPS OVER A 12X10 GRID.
CC
C
       READ(5,1)((((DD(I,J,K,L),I=1,II),J=1,JJ),K=1,KK),L=1,LL)
       READ(5,2)((((VV(I,J,K,L),I=1,II),J=1,JJ),K=1,KK),L=1,LL)
       READ(5,6)((((EE(I,J,K,L),I=1,II),J=1,JJ),K=1,KK),L=1,LL)
C
CC     READ-IN OF SURFACE PRESSURE
CC
C
       READ(5,3)(((PSFC(I,J,L),I=1,II),J=1,JJ),L=1,LL)
C
C
     1 FORMAT(12F5.0)
     2 FORMAT(12F5.0)
     6 FORMAT(12F5.1)
     3 FORMAT(12F5.0)
C
CC     DO LOOP TO COMPUTE VERTICAL PRESSURE LEVELS IN MB
C
       P(1)=950.0
       DO 4 K=2,KK
       P(K)=P(K-1)-50.0
     4 CONTINUE
C
CC     DO LOOP TO CONVERT VV FROM METERS PER SECOND INTO KNOTS
C
       DO 5 L=1,LL
       DO 5 K=1,KK
       DO 5 J=1,JJ
       DO 5 I=1,II
       VV(I,J,K,L)=VV(I,J,K,L)*1.9424
     5 CONTINUE
C
CC     DO LOOP TO ADD 300.0 TO ALL VALUES OF STATIC ENERGY IN (M/S)**2
C
       DO 7 L=1,LL
       DO 7 K=1,KK
       DO 7 J=1,JJ
       DO 7 I=1,II
       EE(I,J,K,L)=EE(I,J,K,L)+300.0
     7 CONTINUE
C
       RETURN
       END
```

```
      SUBROUTINE CONST
C
CCC
CCC   THE PURPOSE OF THIS SUBROUTINE IS TO COMPUTE THE U AND V
CCC   COMPONENTS OF THE WIND IN NAUTICAL MILES PER HOUR, AND TO
CCC   COMPUTE THE CHANGES IN LATITUDE
CCC
C
      COMMON DD(12,10,17,5),VV(12,10,17,5),U(12,10,17,5),V(12,10,17,5),
     1DIV(12,10,17,5),W(12,10,17,5),P(17),PSFC(12,10,5),DX(10),
     2Q(12,10,5),DIVZER(12,10,5),ENG(12,10,17,5),DIVBAR(10,8),
     3WBAR(10,8),ENGBAR(10,8),II,JJ,KK,LL,DY,DT,ILESS,JLESS,KLESS,LLESS,
     4IIESS,JJESS,BL,BLI,PSI,EE(12,10,17,5)
C
CCC   COMPUTATION OF THE U AND V COMPONENTS OF THE WIND:
C
      DO 26 L=1,LL
      DO 26 K=1,KK
      DO 26 J=1,JJ
      DO 26 I=1,II
      U(I,J,K,L)=-VV(I,J,K,L)*SIN(DD(I,J,K,L)*3.14159/180.0)
      V(I,J,K,L)=-VV(I,J,K,L)*COS(DD(I,J,K,L)*3.14159/180.0)
   26 CONTINUE
C
CCC   COMPUTATION OF DELTA X FOR CHANGE IN LATITUDE
C
      PSI=BL*3.14159/180.0
      DO 27 J=1,JJ
      DX(J)=DY*COS(PSI)
      PSI=PSI+BLI*3.14159/180.0
   27 CONTINUE
C
      RETURN
      END


      SUBROUTINE DDOTV
C
CCC
CCC   THE PURPOSE OF THIS SUBROUTINE IS TO COMPUTE THE DIVERGENCE IN
CCC   TERMS OF PER SECOND. THIS IS DONE BY USING A TRAPAZOIDAL
CCC   SMOOTHING FUNCTION BASED ON GAUSES THEOREM.  AFTER DIVERGENCE
CCC   HAS BEEN COMPUTED, AN ERROR TERM, DIVZER, IS COMPUTED WHICH
CCC   CORRECTS THE DIVERGENCE AND THE VERTICAL MOTION (STILL TO BE
CCC   COMPUTED) FOR THE BLOW UP TENDENCY OF THE KINEMATIC METHOD.
CCC   THEN, THE DIVERGENCE IS RECOMPUTED BY SUBTRACTING THE DIVZER TERM.
C     FINALLY, THE VERTICAL SUM OF THE DIVERGENCE TERMS IS COMPUTED.
```

```
      COMMON DD(12,10,17,5),VV(12,10,17,5),U(12,10,17,5),V(12,10,17,5),
     1DIV(12,10,17,5),W(12,10,17,5),P(17),PSFC(12,10,5),DX(10),
     2Q(12,10,5),DIVZER(12,10,5),ENG(12,10,17,5),DIVBAR(10,8),
     3WBAR(10,8),ENGBAR(10,8),II,JJ,KK,LL,DY,DT,ILESS,JLESS,KLESS,LLESS,
     4IIESS,JJESS,BL,BLI,PSI,EE(12,10,17,5)
      COMMON DV1(24),DV2(24),DV3(24),DV4(24),DV5(24),AAA,BBB,CCC,DDD
C
      DIMENSION T1(5),X1(17)
C
      DATA X1/' SFC',' 900',' 850',' 800',' 750',' 700',' 650',' 600',
     1' 550',' 500',' 450',' 400',' 350',' 300',' 250',' 200',' 150'/
      DATA T1/'2300','0030','0200','0330','0500'/
C
C
      AAA=1.0
      BBB=3.0
      CCC=5.0
      DDD=2.0*(AAA+BBB)+CCC
C
CC
CC    READ IN TITLES FOR PRINTING OUT THE FOLLOWING ITEMS:
CC
CC
CC    HORIZONTALLY AREA AVERAGED DIVERGENCE
CC    VERTICALLY AVERAGED DIVERGENCE
CC    DIVERGENCE ERROR
CC    CORRECTED DIVERGENCE
CC    VERTICAL SUM OF THE DIVERGENCE TERMS
CC
C
      READ(5,57)DV1
      READ(5,58)DV2
      READ(5,59)DV3
      READ(5,93)DV4
      READ(5,94)DV5
   57 FORMAT(12A4)
   58 FORMAT(12A4)
   59 FORMAT(12A4)
   93 FORMAT(12A4)
   94 FORMAT(12A4)
C
CC    COMPUTATION OF THE HORIZONTALLY AREA AVERAGED DIVERGENCE USING A
CC    TRAPAZOIDAL SMOOTHING FUNCTION BASED ON GAUSES THEOREM IN PER SEC.
C
      DO 51 L=1,LL
      DO 51 K=1,KK
      DO 51 J=2,JLESS
      DO 51 I=2,ILESS
```

```
      DIV(I,J,K,L)=-1.0/(2.0*DY*(DX(J-1)+DX(J+1)))*((V(I+1,J-1,K,L)+2.0*
     1V(I,J-1,K,L)+V(I-1,J-1,K,L))/4.0*2.0*DX(J-1)-(U(I+1,J+1,K,L)+2.0*
     2U(I+1,J,K,L)+U(I+1,J-1,K,L))/4.0*2.0*DY-(V(I+1,J+1,K,L)+2.0*
     3V(I,J+1,K,L)+V(I-1,J+1,K,L))/4.0*2.0*DX(J+1)+(U(I-1,J+1,K,L)+2.0*
     4U(I-1,J,K,L)+U(I-1,J-1,K,L))/4.0*2.0*DY)
      DIV(I,J,K,L)=DIV(I,J,K,L)/3600.0
   51 CONTINUE
C
CCC
CCC   PRINT OUT OF HORIZONTAL AREA AVERAGED DIVERGENCE IN PER SEC.
CCC
C
      DO 901 L=1,LL
      IA=0
      DO 902 K=1,KK
      DV1(10)=X1(K)
      DV1(17)=T1(L)
      IF(IA-1)201,202,202
  201 IA=1
      GO TO 203
  202 IA=0
      GO TO 204
  203 WRITE(6,92)DV1
   92 FORMAT('1',18X,24A4,//)
      GO TO 904
  204 WRITE(6,921)DV1
  921 FORMAT('0',18X,24A4,//)
      GO TO 904
  904 DO 903 J=2,JLESS
      JJJ=11-J
      WRITE(6,91)JJJ,(DIV(I,JJJ,K,L),I=2,ILESS)
   91 FORMAT(' ',2X,I2,2X,10E11.3,//)
  903 CONTINUE
  902 CONTINUE
  901 CONTINUE
C
CCC
CCC   NOW CALL SUBROUTINE DVERT IN ORDER TO AVERAGE THE
CCC   DIVERGENCE FIELD IN THE VERTICAL
CCC
C
      CALL DVERT
C
CCC
CCC   PRINT OUT OF HORIZONTALLY AND VERTICALLY AVERAGED DIVERGENCE IN
C     UNITS OF PER SECOND.
```

```
      DO 601 L=1,LL
      IB=0
      DO 602 K=1,KK
      DV5(12)=X1(K)
      DV5(19)=T1(L)
      IF(IB-1)301,302,302
  301 IB=1
      GO TO 303
  302 IB=0
      GO TO 304
  303 WRITE(6,61)DV5
   61 FORMAT('1',18X,24A4,//)
      GO TO 604
  304 WRITE(6,611)DV5
  611 FORMAT('0',18X,24A4,//)
      GO TO 604
  604 DO 603 J=2,JLESS
      JJJ=11-J
      WRITE(6,62)JJJ,(DIV(I,JJJ,K,L),I=2,ILESS)
   62 FORMAT(' ',2X,I2,2X,10E11.3,//)
  603 CONTINUE
  602 CONTINUE
  601 CONTINUE
C
CC
CC    ZERO OUT Q(I,J,L) IN ORDER TO USE IN COMPUTATION OF THE DIVERGENCE
CC    ERROR TERM
CC
C
      DO 52 L=1,LL
      DO 52 J=2,JLESS
      DO 52 I=2,ILESS
      Q(I,J,L)=0.0
   52 CONTINUE
C
CC
CC    COMPUTATION OF VERTICAL MOTION AT THE SURFACE IN ORDER TO USE THE
CC    RESULTS IN COMPUTING DIVZER. OMEGA AT THE SURFACE IS COMPUTED
CC    ALLOWING FOR TERRAIN EFFECTS USING THE 950MB WINDS TO REPRESENT
CC    THE SURFACE. UNITS ARE IN MB PER SECOND.
CC
C
      DO 53 L=1,LL
      DO 53 J=2,JLESS
      DO 53 I=2,ILESS
      W(I,J,1,L)=(U(I,J,1,L)*(PSFC(I+1,J,L)-PSFC(I-1,J,L))/(2.0*DX(J))+
     1V(I,J,1,L)*(PSFC(I,J+1,L)-PSFC(I,J-1,L))/(2.0*DY))/3600.0
   53 CONTINUE
```

```
C      COMPUTATION OF DIVZER, ASSUMING THAT ALL THE ERROR IS CONTAINED IN
C      THE OMEGA TERMS DUE TO USING THE CONTINUITY EQUATION.  IT IS
C      ASSUMED THAT OMEGA EQUALS ZERO AT THE 150MB LEVEL OF THE
C      ATMOSPHERE
C
C
C
       DO 54 L=1,LL
       DO 54 J=2,JLESS
       DO 54 I=2,ILESS
       DIVZER(I,J,L)=DIV(I,J,17,L)+2.0*DIV(I,J,16,L)+2.0*DIV(I,J,15,L)+
      12.0*DIV(I,J,14,L)+2.0*DIV(I,J,13,L)+2.0*DIV(I,J,12,L)+2.0*
      2DIV(I,J,11,L)+2.0*DIV(I,J,10,L)+2.0*DIV(I,J,9,L)+2.0*DIV(I,J,8,L)+
      32.0*DIV(I,J,7,L)+2.0*DIV(I,J,6,L)+2.0*DIV(I,J,5,L)+2.0*
      4DIV(I,J,4,L)+2.0*DIV(I,J,3,L)+DIV(I,J,2,L)+(DIV(I,J,2,L)+
      5DIV(I,J,1,L))*(PSFC(I,J,L)-900.0)/50.0+W(I,J,1,L)/25.0
   54 CONTINUE
C
C
C      PRINT OUT OF DIVERGENCE ERROR (DIVZER) FOR EACH TIME STEP
C
C
       DO 63 L=1,LL
       DV2(11)=TI(L)
       WRITE(6,64)DV2
   64  FORMAT('1',18X,24A4,//)
       DO 63 J=2,JLESS
       JJJ=11-J
       WRITE(6,65)JJJ,(DIVZER(I,JJJ,L),I=2,ILESS)
   65  FORMAT(' ',2X,I2,2X,10E11.3,//)
   63  CONTINUE
C
C      COMPUTATION OF CORRECTED DIVERGENCE USING DIVZER.  THIS ALLOWS
C      FOR MINIMIZING THE OMEGA FIELD AT 150 MB.
C
C
       DO 55 L=1,LL
       DO 55 J=2,JLESS
       DO 55 I=2,ILESS
       Q(I,J,L)=DIVZER(I,J,L)/((PSFC(I,J,L)-150.0)*0.04)
   55  CONTINUE
       DO 56 L=1,LL
       DO 56 K=1,KK
       DO 56 J=2,JLESS
       DO 56 I=2,ILESS
       DIV(I,J,K,L)=DIV(I,J,K,L)-Q(I,J,L)
   56  CONTINUE
```

```
C      PRINT OUT OF CORRECTED AREA AVERAGED DIVERGENCE
C
       DO 661 L=1,LL
       IC=0
       DO 662 K=1,KK
       DV3(13)=X1(K)
       DV3(20)=T1(L)
       IF(IC-1)401,402,402
  401  IC=1
       GO TO 403
  402  IC=0
       GO TO 404
  403  WRITE(6,67)DV3
   67  FORMAT('1',18X,24A4,//)
       GO TO 664
  404  WRITE(6,671)DV3
  671  FORMAT('0',18X,24A4,//)
       GO TO 664
  664  DO 663 J=2,JLESS
       JJJ=11-J
       WRITE(6,68)JJJ,(DIV(I,JJJ,K,L),I=2,ILESS)
   68  FORMAT(' ',2X,I2,2X,10E11.3,//)
  663  CONTINUE
  662  CONTINUE
  661  CONTINUE
C
C
C      NOW CALL SUBROUTINE DSUM IN ORDER TO VERTICALLY ADD
C      THE DIVERGENCE FIELD IN EACH COLUMN
C
       CALL DSUM
C
       RETURN
       END


       SUBROUTINE DVERT
C
C      THE PURPOSE OF THIS SUBROUTINE IS TO SMOOTH THE DIVERGENCE FIELD
C      IN THE VERTICAL AND UPON COMPLETION RETURN TO SUBROUTINE DDOTV
C      TO COMPLETE THAT SUBROUTINE
C
       COMMON DD(12,10,17,5),VV(12,10,17,5),U(12,10,17,5),V(12,10,17,5),
      1DIV(12,10,17,5),W(12,10,17,5),P(17),PSFC(12,10,5),DX(10),
      2Q(12,10,5),DIVZER(12,10,5),ENG(12,10,17,5),DIVBAR(10,8),
      3WBAR(10,8),ENGBAR(10,8),II,JJ,KK,LL,DY,DT,ILESS,JLESS,KLESS,LLESS,
      4IIESS,JJESS,BL,BLI,PSI,EE(12,10,17,5)
       COMMON DV1(24),DV2(24),DV3(24),DV4(24),DV5(24),AAA,BBB,CCC,DDD
```

```
C      IT IS NOW NECESSARY TO SMOOTH THE DIVERGENCE FIELD IN THE VERTICAL
C      USING A TECHNIQUE SIMILAR TO THE FOLLOWING:
C
C
C                        *****                       *****
C                        * B *          K+1          * B *
C                     ****   ****                 ****   ****
C                     * A  C  A *       K         * A  C  A *
C                     ****   ****                 ****   ****
C                        * B *          K-1          * B *
C                        *****                       *****
C                      I-1 I I+1                   J-1 J J+1
C
C
C
C      FIRST, SMOOTH ALL POINTS FROM K=2,16, I=3,10, AND J=3,8
C
C
       DO 70 L=1,LL
       DO 70 K=2,KLESS
       DO 70 J=3,JJESS
       DO 70 I=3,IIESS
       DIV(I,J,K,L)=(2.0*(BBB*(DIV(I,J,K+1,L)+DIV(I,J,K-1,L))+CCC*
      1DIV(I,J,K,L))+AAA*(DIV(I-1,J,K,L)+DIV(I+1,J,K,L)+DIV(I,J-1,K,L)+
      2DIV(I,J+1,K,L)))/(2.0*DDD)
    70 CONTINUE
C
C
C      NOW SMOOTH THE POINTS AT K=1 AND 17 FOR I=3,10 AND J=3,8
C
C
       DO 71 L=1,LL
       DO 71  J=3,JJESS
       DO 71  I=3,IIESS
       DIV(I,J,1,L)=(2.0*(BBB*(DIV(I,J,3,L)+DIV(I,J,2,L))+CCC*DIV(I,J,1,
      1L))+AAA*(DIV(I-1,J,2,L)+DIV(I+1,J,2,L)+DIV(I,J-1,2,L)+DIV(I,J+1,
      22,L)))/(2.0*DDD)
       DIV(I,J,17,L)=(2.0*(BBB*(DIV(I,J,15,L)+DIV(I,J,16,L))+CCC*DIV(I,J,
      117,L))+AAA*(DIV(I-1,J,16,L)+DIV(I+1,J,16,L)+DIV(I,J-1,16,L)+DIV(I,
      2J+1,16,L)))/(2.0*DDD)
    71 CONTINUE
C
C
C      THIS NOW COMPLETES THE SMOOTHING OF ALL OF THE INTERIOR POINTS
C      FRCM THE SURFACE TO 150 MB
C
C
C
C      SMOOTH THE POINTS AT J=2 AND 9 FOR K=2,16 AND I=3,10
C
```

```
      DO 72 L=1,LL
      DO 72 K=2,KLESS
      DO 72 I=3,IIESS
      DIV(I,2,K,L)=(2.0*(BBB*(DIV(I,2,K+1,L)+DIV(I,2,K-1,L))+CCC*DIV(I,
     12,K,L))+AAA*(DIV(I-1,2,K,L)+DIV(I+1,2,K,L)+DIV(I,3,K,L)))/(2.0*
     2DDD-AAA)
      DIV(I,9,K,L)=(2.0*(BBB*(DIV(I,9,K+1,L)+DIV(I,9,K-1,L))+CCC*
     1DIV(I,9,K,L))+AAA*(DIV(I-1,9,K,L)+DIV(I+1,9,K,L)+DIV(I,8,K,
     2L)))/(2.0*DDD-AAA)
   72 CONTINUE
C
CCCC
      SMOOTH THE POINTS AT I=2 AND 11 FOR K=2,16 AND J=3,8
CCCC
C
      DO 73 L=1,LL
      DO 73 K=2,KLESS
      DO 73 J=3,JJESS
      DIV(2,J,K,L)=(2.0*(BBB*(DIV(2,J,K+1,L)+DIV(2,J,K-1,L))+CCC*DIV(2,
     1J,K,L))+AAA*(DIV(2,J-1,K,L)+DIV(2,J+1,K,L)+DIV(3,J,K,L)))/(2.0*
     2DDD-AAA)
      DIV(11,J,K,L)=(2.0*(BBB*(DIV(11,J,K+1,L)+DIV(11,J,K-1,L))+CCC*
     1DIV(11,J,K,L))+AAA*(DIV(11,J-1,K,L)+DIV(11,J+1,K,L)+DIV(10,J,K,
     2L)))/(2.0*DDD-AAA)
   73 CONTINUE
C
CCCC
      NOW SMOOTH THE POINTS AT J=2 AND 9 FOR K=1 AND 17 AND I=3,10
CCCC
C
      DO 74 L=1,LL
      DO 74 I=3,IIESS
      DIV(I,2,1,L)=(2.0*(BBB*(DIV(I,2,3,L)+DIV(I,2,2,L))+CCC*DIV(I,2,1,
     11,L))+AAA*(DIV(I-1,2,2,L)+DIV(I+1,2,2,L)+DIV(I,3,2,L)))/(2.0*DDD-
     2AAA)
      DIV(I,9,1,L)=(2.0*(BBB*(DIV(I,9,3,L)+DIV(I,9,2,L))+CCC*DIV(I,
     19,1,L))+AAA*(DIV(I-1,9,2,L)+DIV(I+1,9,2,L)+DIV(I,8,2,L)))/(2.0*
     2DDD-AAA)
      DIV(I,2,17,L)=(2.0*(BBB*(DIV(I,2,15,L)+DIV(I,2,16,L))+CCC*DIV(I,2,
     117,L))+AAA*(DIV(I-1,2,16,L)+DIV(I+1,2,16,L)+DIV(I,3,16,L)))/(2.0*
     2DDD-AAA)
      DIV(I,9,17,L)=(2.0*(BBB*(DIV(I,9,15,L)+DIV(I,9,16,L))+CCC*
     1DIV(I,9,17,L))+AAA*(DIV(I-1,9,16,L)+DIV(I+1,9,16,L)+DIV(I,8,16,
     2L)))/(2.0*DDD-AAA)
   74 CONTINUE
C
CCC
      NOW SMOOTH THE POINTS AT I=2 AND 11 FOR K=1 AND 17 AND J=3,8
```

```
      DO 75 L=1,LL
      DO 75 J=3,JJESS
      DIV(2,J,1,L)=(2.0*(BBB*(DIV(2,J,3,L)+DIV(2,J,2,L))+CCC*DIV(2,J,1,
     1L))+AAA*(DIV(2,J+1,2,L)+DIV(2,J-1,2,L)+DIV(3,J,2,L)))/(2.0*DDD-
     2AAA)
      DIV(11,J,1,L)=(2.0*(BBB*(DIV(11,J,3,L)+DIV(11,J,2,L))+CCC*DIV(11,
     1J,1,L))+AAA*(DIV(11,J+1,2,L)+DIV(11,J-1,2,L)+DIV(10,J,2,L)))/(2.0*
     2DDD-AAA)
      DIV(2,J,17,L)=(2.0*(BBB*(DIV(2,J,15,L)+DIV(2,J,16,L))+CCC*DIV(2,J,
     117,L))+AAA*(DIV(2,J+1,16,L)+DIV(2,J-1,16,L)+DIV(3,J,16,L)))/(2.0*
     2DDD-AAA)
      DIV(11,J,17,L)=(2.0*(BBB*(DIV(11,J,15,L)+DIV(11,J,16,L))+CCC*
     1DIV(11,J,17,L))+AAA*(DIV(11,J+1,16,L)+DIV(11,J-1,16,L)+DIV(10,J,
     216,L)))/(2.0*DDD-AAA)
   75 CONTINUE
C
C     THIS NOW COMPLETES THE SMOOTHING OF ALL POINTS EXCEPT AT THE
C     FOUR CORNERS
C
C     NOW SMOOTH THE POINTS FROM K=2,16 AT J=2 AND 9 AND I=2 AND 11
C
      DO 76 L=1,LL
      DO 76 K=2,KLESS
      DIV(2,2,K,L)=(2.0*(BBB*(DIV(2,2,K+1,L)+DIV(2,2,K-1,L))+CCC*DIV(2,
     12,K,L))+AAA*(DIV(2,3,K,L)+DIV(3,2,K,L)))/(2.0*(DDD-AAA))
      DIV(2,9,K,L)=(2.0*(BBB*(DIV(2,9,K+1,L)+DIV(2,9,K-1,L))+CCC*
     1DIV(2,9,K,L))+AAA*(DIV(2,8,K,L)+DIV(3,9,K,L)))/(2.0*(DDD-AAA))
      DIV(11,2,K,L)=(2.0*(BBB*(DIV(11,2,K+1,L)+DIV(11,2,K-1,L))+CCC*
     1DIV(11,2,K,L))+AAA*(DIV(11,3,K,L)+DIV(10,2,K,L)))/(2.0*(DDD-AAA))
      DIV(11,9,K,L)=(2.0*(BBB*(DIV(11,9,K+1,L)+DIV(11,9,K-1,L))+CCC*
     1DIV(11,9,K,L))+AAA*(DIV(11,8,K,L)+DIV(10,9,K,L)))/(2.0*(DDD-AAA))
   76 CONTINUE
C
C     FINALLY, SMOOTH THE POINTS AT K=1 AND 17 FOR J=2 AND 9 AND I=2
C     AND 11
C
      DO 77 L=1,LL
      DIV(2,2,1,L)=(2.0*(BBB*(DIV(2,2,3,L)+DIV(2,2,2,L))+CCC*DIV(2,2,1,
     1L))+AAA*(DIV(2,3,2,L)+DIV(3,2,2,L)))/(2.0*(DDD-AAA))
      DIV(2,9,1,L)=(2.0*(BBB*(DIV(2,9,3,L)+DIV(2,9,2,L))+CCC*DIV(2,
     19,1,L))+AAA*(DIV(2,8,2,L)+DIV(3,9,2,L)))/(2.0*(DDD-AAA))
      DIV(11,2,1,L)=(2.0*(BBB*(DIV(11,2,3,L)+DIV(11,2,2,L))+CCC*DIV(11,
     12,1,L))+AAA*(DIV(11,3,2,L)+DIV(10,2,2,L)))/(2.0*(DDD-AAA))
      DIV(11,9,1,L)=(2.0*(BBB*(DIV(11,9,3,L)+DIV(11,9,2,L))+CCC*DIV(11,
     19,1,L))+AAA*(DIV(11,8,2,L)+DIV(10,9,2,L)))/(2.0*(DDD-AAA))
```

```
      DIV(2,2,17,L)=(2.0*(BBB*(DIV(2,2,15,L)+DIV(2,2,16,L))+CCC*DIV(2,2,
     117,L))+AAA*(DIV(2,3,16,L)+DIV(3,2,16,L)))/(2.0*(DDD-AAA))
      DIV(2,9,17,L)=(2.0*(BBB*(DIV(2,9,15,L)+DIV(2,9,16,L))+CCC*DIV(2,9,
     117,L))+AAA*(DIV(2,8,16,L)+DIV(3,9,16,L)))/(2.0*(DDD-AAA))
      DIV(11,2,17,L)=(2.0*(BBB*(DIV(11,2,15,L)+DIV(11,2,16,L))+CCC*
     1DIV(11,2,17,L))+AAA*(DIV(11,3,16,L)+DIV(10,2,16,L)))/(2.0*(DDD-
     2AAA))
      DIV(11,9,17,L)=(2.0*(BBB*(DIV(11,9,15,L)+DIV(11,9,16,L))+CCC*
     1DIV(11,9,17,L))+AAA*(DIV(11,8,16,L)+DIV(10,9,16,L)))/(2.0*(DDD-
     2AAA))
   77 CONTINUE
C
CC      THIS COMPLETES ALL SMOOTHING FOR THE DIVERGENCE, BOTH IN THE
CC      HORIZONTAL AND IN THE VERTICAL.
C
        RETURN
        END


        SUBROUTINE DSUM
C
CCC
CCC     THE PURPOSE OF THIS SUBROUTINE IS TO VERTICALLY ADD THE CORRECTED
CC      VERTICALLY AND HORIZONTALLY SMOOTHED DIVERGENCE IN ORDER TO SEE
CC      IF IT IS SYMMETRICAL ABOUT THE K AXIS
CC
C
        COMMON DD(12,10,17,5),VV(12,10,17,5),U(12,10,17,5),V(12,10,17,5),
     1DIV(12,10,17,5),W(12,10,17,5),P(17),PSFC(12,10,5),DX(10),
     2Q(12,10,5),DIVZER(12,10,5),ENG(12,10,17,5),DIVBAR(10,8),
     3WBAR(10,8),ENGBAR(10,8),II,JJ,KK,LL,DY,DT,ILESS,JLESS,KLESS,LLESS,
     4IIESS,JJESS,BL,BLI,PSI,EE(12,10,17,5)
        COMMON DV1(24),DV2(24),DV3(24),DV4(24),DV5(24),AAA,BBB,CCC,DDD
C
        DIMENSION T1(5)
C
        DATA T1/'2300','0030','0200','0330','0500'/
C
CC      ZERO OUT THE DIVZER TERM
C
        DO 85 L=1,LL
        DO 85 J=2,JLESS
        DO 85 I=2,ILESS
        DIVZER(I,J,L)=0.0
   85 CONTINUE
C
CC      COMPUTE THE VERTICAL SUM OF THE DIVERGENCE
```

```
      DO 86 L=1,LL
      DO 86 J=2,JLESS
      DO 86 I=2,ILESS
      DO 86 K=1,KK
      DIVZER(I,J,L)=DIVZER(I,J,L)+DIV(I,J,K,L)
   86 CONTINUE
C
CCC   PRINT OUT OF THE DIVZER TERM
C
      DO 87 L=1,LL
      DV4(9)=T1(L)
      WRITE(6,88)DV4
   88 FORMAT('1',18X,24A4,//)
      DO 87 J=2,JLESS
      JJJ=11-J
      WRITE(6,89)JJJ,(DIVZER(I,JJJ,L),I=2,ILESS)
   89 FORMAT(' ',2X,I2,2X,10E11.3,//)
   87 CONTINUE
C
CCC   RETURN TO SUBROUTINE DDOTV
C
      RETURN
      END


      SUBROUTINE OMEGA
C
CCCCC
CCCCC THE PURPOSE OF THIS SUBROUTINE IS TO COMPUTE OMEGA THROUGH 17
CCCCC LEVELS OF THE ATMOSPHERE FOR 5 TIME STEPS, ASSUMING OMEGA AT
CCCCC 150MB IS EQUAL TO ZERO. OMEGA AT THE SURFACE WAS COMPUTED IN
CCCCC SUBROUTINE DDOTV.
CCCCC
CCCCC ONCE OMEGA IS COMPUTED FOR ALL LEVELS AND TIME STEPS, IT IS TO
CCCCC BE PRINTED OUT IN ORDER TO SEE IF THE BOUNDARY CONDITIONS HELD
CCCCC FOR OMEGA AT 150MB, THAT IS, WAS DIVZER CORRECTLY COMPUTED
C
      COMMON DD(12,10,17,5),VV(12,10,17,5),U(12,10,17,5),V(12,10,17,5),
     1DIV(12,10,17,5),W(12,10,17,5),P(17),PSFC(12,10,5),DX(10),
     2Q(12,10,5),DIVZER(12,10,5),ENG(12,10,17,5),DIVBAR(10,8),
     3WBAR(10,8),ENGBAR(10,8),II,JJ,KK,LL,DY,DT,ILESS,JLESS,KLESS,LLESS,
     4IIESS,JJESS,BL,BLI,PSI,EE(12,10,17,5)
C
      DIMENSION DV6(24),X1(17),T1(5)
C
      DATA X1/' SFC',' 900',' 850',' 800',' 750',' 700',' 650',' 600',
     1' 550',' 500',' 450',' 400',' 350',' 300',' 250',' 200',' 150'/
      DATA T1/'2300','0030','0200','0330','0500'/
```

```
C      COMPUTE VERTICAL MOTION USING THE CONTINUITY EQUATION. OMEGA FOR
CC     THE SURFACE WAS COMPUTED IN SUBROUTINE DDOTV
C
       DO 100 L=1,LL
       DO 100 K=1,KLESS
       DO 100 J=2,JLESS
       DO 100 I=2,ILESS
       IF(K.EQ.1) GO TO 105
       GO TO 106
  105 W(I,J,K+1,L)=W(I,J,K,L)+(DIV(I,J,K+1,L)+DIV(I,J,K,L))/2.0*
     1(PSFC(I,J,L)-P(K+1))
       GO TO 100
  106 W(I,J,K+1,L)=W(I,J,K,L)+(DIV(I,J,K+1,L)+DIV(I,J,K,L))/2.0*
     1(P(K)-P(K+1))
  100 CONTINUE
C
CC     READ IN OF TITLE FOR PRINTING OUT VALUES OF OMEGA
C
       READ(5,101)DV6
  101 FORMAT(12A4)
C
CC
CCC    PRINT OUT OF VERTICAL MOTION FOR 17 LEVELS OF THE ATMOSPHERE AND
CC     5 TIME STEPS IN MB/SEC.  DOES OMEGA AT 150MB EQUAL ZERO?
C
       DO 1021 L=1,LL
       ID=0
       DO 1022 K=1,KK
       DV6(13)=X1(K)
       DV6(20)=T1(L)
       IF(ID-1)501,502,502
  501  ID=1
       GO TO 503
  502  ID=0
       GO TO 504
  503  WRITE(6,103)DV6
  103  FORMAT('1',18X,24A4,//)
       GO TO 1024
  504  WRITE(6,1031)DV6
 1031  FORMAT('0',18X,24A4,//)
       GO TO 1024
 1024  DO 1023 J=2,JLESS
       JJJ=11-J
       WRITE(6,104)JJJ,(W(I,JJJ,K,L),I=2,ILESS)
  104  FORMAT(' ',2X,I2,2X,10E11.3,//)
 1023  CONTINUE
 1022  CONTINUE
 1021  CONTINUE
```

```
      RETURN
      END


      SUBROUTINE ENERGY
C
CCC   THE PURPOSE OF THIS SUBROUTINE IS TO COMPUTE THE TOTAL
CCC   DERIVATIVE OF STATIC ENERGY IN ORDER TO DETERMINE IF THE
CC    STATIC ENERGY IS TOTALLY CONSERVED, THAT IS:
C                              DOES DE/DT=0?
CCC   WHERE:
CCC   STATIC ENERGY, E=(CP*T+G*Z+L*Q) IN JOULES/GM=10**3*(M/S)**2 AND
CCC   CP=SPECIFIC HEAT AT CONSTANT PRESSURE
CCC   T= ABSOLUTE TEMPERATURE
CCC   G= ACCELERATION OF GRAVITY
CCC   Z=HEIGHT IN METERS
CCC   L=LATENT HEAT OF VAPORIZATION
CCC   Q=ACTUAL MIXING RATIO IN GM/KG
CCC
C
      COMMON DD(12,10,17,5),VV(12,10,17,5),U(12,10,17,5),V(12,10,17,5),
     1DIV(12,10,17,5),W(12,10,17,5),P(17),PSFC(12,10,5),DX(10),
     2Q(12,10,5),DIVZER(12,10,5),ENG(12,10,17,5),DIVBAR(10,8),
     3WBAR(10,8),ENGBAR(10,8),II,JJ,KK,LL,DY,DT,ILESS,JLESS,KLESS,LLESS,
     4IIESS,JJESS,BL,BLI,PSI,EE(12,10,17,5)
C
      DIMENSION DV9(24),X1(17),T1(5)
C
      DATA X1/' SFC',' 900',' 850',' 800',' 750',' 700',' 650',' 600',
     1' 550',' 500',' 450',' 400',' 350',' 300',' 250',' 200',' 150'/
      DATA T1/'2300','0030','0200','0330','0500'/
C
CCC   COMPUTE THE TOTAL DERIVATIVE OF THE STATIC ENERGY FROM K=3 TO 16
CC    USING CENTERED DIFFERENCES.
C
      DO 175 L=2,LLESS
      DO 175 K=3,KLESS
      DO 175 J=2,JLESS
      DO 175 I=2,ILESS
      ENG(I,J,K,L)=((EE(I,J,K,L+1)-EE(I,J,K,L-1))/(2.0*DT)+(U(I,J,K,
     1L)*(EE(I+1,J,K,L)-EE(I-1,J,K,L))/(2.0*DX(J))+V(I,J,K,L)*(EE(I,
     2J+1,K,L)-EE(I,J-1,K,L))/(2.0*DY))/3600.0+W(I,J,K,L)*(EE(I,J,K-1,
     3L)-EE(I,J,K+1,L))/100.0)*5.4
  175 CONTINUE
C
CC    COMPUTE THE TOTAL DERIVATIVE OF THE STATIC ENERGY AT K=2 USING
C     CENTERED DIFFERENCES
```

```
      DO 176 L=2,LLESS
      DO 176 J=2,JLESS
      DO 176 I=2,ILESS
      ENG(I,J,2,L)=((EE(I,J,2,L+1)-EE(I,J,2,L-1))/(2.0*DT)+(U(I,J,2,
     1L)*(EE(I+1,J,2,L)-EE(I-1,J,2,L))/(2.0*DX(J))+V(I,J,2,L)*(EE(I,
     2J+1,2,L)-EE(I,J-1,2,L))/(2.0*DY))/3600.0+W(I,J,2,L)*(EE(I,J,1,
     3L)-EE(I,J,3,L))/(PSFC(I,J,L)-P(3)))*5.4
  176 CONTINUE
C
CC    COMPUTE DE/DT AT K=1 USING FORWARD DIFFERENCING FOR THE PRESSURE
CC    TERM AND CENTERED DIFFERENCING FOR THE OTHER PARTIALS
C
      DO 177 L=2,LLESS
      DO 177 J=2,JLESS
      DO 177 I=2,ILESS
      ENG(I,J,1,L)=((EE(I,J,1,L+1)-EE(I,J,1,L-1))/(2.0*DT)+(U(I,J,1,
     1L)*(EE(I+1,J,1,L)-EE(I-1,J,1,L))/(2.0*DX(J))+V(I,J,1,L)*(EE(I,
     2J+1,1,L)-EE(I,J-1,1,L))/(2.0*DY))/3600.0+W(I,J,1,L)*(EE(I,J,1,
     3L)-EE(I,J,2,L))/(PSFC(I,J,L)-P(2)))*5.4
  177 CONTINUE
C
CC    FINALLY, COMPUTE DE/DT AT K=17 USING BACKWARD DIFFERENCING FOR THE
CC    PRESSURE TERM AND CENTERED DIFFERENCING FOR THE OTHER PARTIALS
C
      DO 178 L=2,LLESS
      DO 178 J=2,JLESS
      DO 178 I=2,ILESS
      ENG(I,J,17,L)=((EE(I,J,17,L+1)-EE(I,J,17,L-1))/(2.0*DT)+(U(I,J,
     117,L)*(EE(I+1,J,17,L)-EE(I-1,J,17,L))/(2.0*DX(J))+V(I,J,17,L)*
     2(EE(I,J+1,17,L)-EE(I,J-1,17,L))/(2.0*DY))/3600.0+W(I,J,17,L)*
     3(EE(I,J,16,L)-EE(I,J,17,L))/50.0)*5.4
  178 CONTINUE
C
CC    THIS COMPLETES THE COMPUTATION OF THE TOTAL DERIVATIVE OF STATIC
CC    ENERGY.  NOW TO PRINT OUT THE RESULTS.
CC
CC    FIRST, READ IN THE TITLE FOR THE STATIC ENERGY.
C
      READ(5,179)DV9
  179 FORMAT(12A4)
C
      DO 180 L=2,LLESS
      IE=0
      DO 181 K=1,KK
      DV9(14)=X1(K)
      DV9(18)=T1(L)
      IF(IE-1)601,602,602
  601 IE=1
```

```
      GO TO 603
  602 IE=0
      GO TO 604
  603 WRITE(6,183)DV9
  183 FORMAT('1',18X,24A4,//)
      GO TO 185
  604 WRITE(6,184)DV9
  184 FORMAT('0',18X,24A4,//)
      GO TO 185
  185 DO 182 J=2,JLESS
      JJJ=11-J
      WRITE(6,186)JJJ,(ENG(I,JJJ,K,L),I=2,ILESS)
  186 FORMAT(' ',2X,I2,2X,10E11.3,//)
  182 CONTINUE
  181 CONTINUE
  180 CONTINUE
C
      RETURN
      END


      SUBROUTINE PRNT1
C
CCCCC
CCCCC     THE PURPOSE OF THIS SUBROUTINE IS TO TAKE THE PREVIOUSLY
CCCCC     COMPUTED VALUES FOR THE CORRECTED DIVERGENCE, VERTICAL MOTION,
CCCCC     AND CHANGE OF STATIC ENERGY, AND PRINT THEM OUT IN MTMPII
CCCCC     FORMAT IN ORDER TO OBSERVE THEIR PATTERNS ON A CONSTANT PRESSURE
CCCCC     SURFACE
CCC
      COMMON DD(12,10,17,5),VV(12,10,17,5),U(12,10,17,5),V(12,10,17,5),
     1DIV(12,10,17,5),W(12,10,17,5),P(17),PSFC(12,10,5),DX(10),
     2Q(12,10,5),DIVZER(12,10,5),ENG(12,10,17,5),DIVBAR(10,8),
     3WBAR(10,8),ENGBAR(10,8),II,JJ,KK,LL,DY,DT,ILESS,JLESS,KLESS,LLESS,
     4IIESS,JJESS,BL,BLI,PSI,EE(12,10,17,5)
C
CC
      DIMENSION X1(17),T1(5),DV7(24),DV8(24),DV10(24)
CC
CC
      DATA X1/' SFC',' 900',' 850',' 800',' 750',' 700',' 650',' 600',
     1' 550',' 500',' 450',' 400',' 350',' 300',' 250',' 200',' 150'/
      DATA T1/'2300','0030','0200','0330','0500'/
C
CCC
C     READ IN OF TITLES FOR USE IN METMAPPING
```

```
      READ(5,150)DV7
      READ(5,151)DV8
      READ(5,160)DV10
  150 FORMAT(12A4)
  151 FORMAT(12A4)
  160 FORMAT(12A4)
C
CC    IN ORDER TO PRINT OUT THE VALUES IN A MTMPII FORMAT IT IS FIRST
C     NECESSARY TO REDUCE THE GRID SIZES
CC
CC    FIRST, REDUCE THE DIVERGENCE GRID SIZE AND PLACE IN MTMPII FORMAT
C
      DO 152 L=1,LL
      DO 152 K=1,KK
      DO 154 J=1,JJESS
      DO 154 I=1,IIESS
  154 DIVBAR(I,J)=DIV(I+1,J+1,K,L)*10.0**4
      DV7(6)=X1(K)
      DV7(18)=T1(L)
      CALL MTMPII(DIVBAR,10,8,DV7,0.2,0,0,0,0,1)
  152 CONTINUE
C
CC    NOW, REDUCE THE VERTICAL MOTION FIELD GRID SIZE AND PLACE IN A
C     MTMPII FORMAT
C
      DO 153 L=1,LL
      DO 153 K=1,KK
      DO 155 J=1,JJESS
      DO 155 I=1,IIESS
  155 WBAR(I,J)=W(I+1,J+1,K,L)*10.0**2
      DV8(6)=X1(K)
      DV8(18)=T1(L)
      CALL MTMPII(WBAR,10,8,DV8,0.2,0,0,0,0,1)
  153 CONTINUE
C
CC
CC    FINALLY, REDUCE THE TOTAL DERIVATIVE OF STATIC ENERGY AND PLACE
C     IN A MTMPII FORMAT
C
      DO 161 L=2,LLESS
      DO 161 K=1,KK
      DO 162 J=1,JJESS
      DO 162 I=1,IIESS
  162 ENGBAR(I,J)=ENG(I+1,J+1,K,L)*10.0**2
      DV10(10)=X1(K)
      DV10(13)=T1(L)
      CALL MTMPII(ENGBAR,10,8,DV10,0.2,0,0,0,0,1)
  161 CONTINUE
```

```
C     THIS PLACES ALL DESIRED VALUES IN A 1X1 INCH CONTOURED MTMPII
C     REPRESENTATION
C
      RETURN
      END


      SUBROUTINE ADVCT
C
C
C     HAVING ALREADY COMPUTED THE TOTAL DERIVATIVE OF STATIC ENERGY,
C     AND ASSUMING IT TO BE ZERO, IT IS DESIRED TO DETERMINE THE LOCAL
C     RATE OF CHANGE OF STATIC ENERGY BY SETTING IT EQUAL TO THE
C     NEGATIVE VALUE OF THE ADVECTIVE TERMS.
C
C
      COMMON DD(12,10,17,5),VV(12,10,17,5),U(12,10,17,5),V(12,10,17,5),
     1DIV(12,10,17,5),W(12,10,17,5),P(17),PSFC(12,10,5),DX(10),
     2Q(12,10,5),DIVZER(12,10,5),ENG(12,10,17,5),DIVBAR(10,8),
     3WBAR(10,8),ENGBAR(10,8),II,JJ,KK,LL,DY,DT,ILESS,JLESS,KLESS,LLESS,
     4IIESS,JJESS,BL,BLI,PSI,EE(12,10,17,5)
C
      DIMENSION DV9(24),X1(17),T1(5)
C
      DATA X1/' SFC',' 900',' 850',' 800',' 750',' 700',' 650',' 600',
     1' 550',' 500',' 450',' 400',' 350',' 300',' 250',' 200',' 150'/
      DATA T1/'2300','0030','0200','0330','0500'/
C
C
C     COMPUTE THE LOCAL RATE OF CHANGE OF STATIC ENERGY FROM K=3 TO 16
C     USING CENTERED DIFFERENCES.
C
C
      DO 175 L=1,LL
      DO 175 K=3,KLESS
      DO 175 J=2,JLESS
      DO 175 I=2,ILESS
      ENG(I,J,K,L)=                                          ((U(I,J,K,
     1L)*(EE(I+1,J,K,L)-EE(I-1,J,K,L))/(2.0*DX(J))+V(I,J,K,L)*(EE(I,
     2J+1,K,L)-EE(I,J-1,K,L))/(2.0*DY))/3600.0+W(I,J,K,L)*(EE(I,J,K-1,
     3L)-EE(I,J,K+1,L))/100.0)*5.4
      ENG(I,J,K,L)=-ENG(I,J,K,L)
  175 CONTINUE
C
C
C     COMPUTE THE LOCAL RATE OF CHANGE OF STATIC ENERGY AT K=2 USING
C     CENTERED DIFFERENCES
```

```
      DO 176 L=1,LL
      DO 176 J=2,JLESS
      DO 176 I=2,ILESS
      ENG(I,J,2,L)=                                                    ((U(I,J,2,
     1L)*(EE(I+1,J,2,L)-EE(I-1,J,2,L))/(2.0*DX(J))+V(I,J,2,L)*(EE(I,
     2J+1,2,L)-EE(I,J-1,2,L))/(2.0*DY))/3600.0+W(I,J,2,L)*(EE(I,J,3,
     3L)-EE(I,J,1,L))/(PSFC(I,J,L)-P(3)))*5.4
      ENG(I,J,2,L)=-ENG(I,J,2,L)
  176 CONTINUE
C
CCC   COMPUTE THE LOCAL RATE OF CHANGE OF STATIC ENERGY USING FORWARD
CCC   DIFFERENCING FOR THE PRESSURE TERM AND CENTERED DIFFERENCING FOR
CCC   THE OTHER PARTIALS
C
      DO 177 L=1,LL
      DO 177 J=2,JLESS
      DO 177 I=2,ILESS
      ENG(I,J,1,L)=                                                    ((U(I,J,1,
     1L)*(EE(I+1,J,1,L)-EE(I-1,J,1,L))/(2.0*DX(J))+V(I,J,1,L)*(EE(I,
     2J+1,1,L)-EE(I,J-1,1,L))/(2.0*DY))/3600.0+W(I,J,1,L)*(EE(I,J,2,
     3L)-EE(I,J,1,L))/(PSFC(I,J,L)-P(2)))*5.4
      ENG(I,J,1,L)=-ENG(I,J,1,L)
  177 CONTINUE
C
CCC   FINALLY, COMPUTE THE LOCAL RATE OF CHANGE OF STATIC ENERGY AT
CCC   K=17 USING BACKWORD DIFFERENCING FOR THE PRESSURE TERM AND
CCC   CENTERED DIFFERENCING FOR THE OTHER PARTIALS
CCC
      DO 178 L=1,LL
      DO 178 J=2,JLESS
      DO 178 I=2,ILESS
      ENG(I,J,17,L)=                                                   ((U(I,J,
     117,L)*(EE(I+1,J,17,L)-EE(I-1,J,17,L))/(2.0*DX(J))+V(I,J,17,L)*
     2(EE(I,J+1,17,L)-EE(I,J-1,17,L))/(2.0*DY))/3600.0+W(I,J,17,L)*
     3(EE(I,J,17,L)-EE(I,J,16,L))/50.0)*5.4
      ENG(I,J,17,L)=-ENG(I,J,17,L)
  178 CONTINUE
C
CCCCC
CCCCC THIS COMPLETES THE COMPUTATION OF THE LOCAL RATE OF CHANGE OF
CCCCC THE STATIC ENERGY.  NOW TO PRINT OUT THE RESULTS.
CCCCC
CCCCC FIRST, READ IN THE TITLE FOR THE LOCAL RATE OF CHANGE.
CCC
      READ(5,179)DV9
  179 FORMAT(12A4)
```

```
      DO 180 L=1,LL
      IE=0
      DO 181 K=1,KK
      DV9(11)=X1(K)
      DV9(14)=T1(L)
      IF(IE-1)601,602,602
  601 IE=1
      GO TO 603
  602 IE=0
      GO TO 604
  603 WRITE(6,183)DV9
  183 FORMAT('1',18X,24A4,//)
      GO TO 185
  604 WRITE(6,184)DV9
  184 FORMAT('0',18X,24A4,//)
      GO TO 185
  185 DO 182 J=2,JLESS
      JJJ=11-J
      WRITE(6,186)JJJ,(ENG(I,JJJ,K,L),I=2,ILESS)
  186 FORMAT(' ',2X,I2,2X,10E11.3,//)
  182 CONTINUE
  181 CONTINUE
  180 CONTINUE
C
CCC
      NOW MTMPII THE LOCAL RATE OF CHANGE OF STATIC ENERGY
C
      DO 161 L=1,LL
      DO 161 K=1,KK
      DO 162 J=1,JJESS
      DO 162 I=1,IIESS
  162 ENGBAR(I,J)=ENG(I+1,J+1,K,L)*10.0**2
      DV9(11)=X1(K)
      DV9(14)=T1(L)
      CALL MTMPII(ENGBAR,10,8,DV9,0.2,0,0,0,0,1)
  161 CONTINUE
C
      RETURN
      END

      SUBROUTINE PROG
C
CCC
C     THE PURPOSE OF THIS SUBROUTINE IS TO METMAP THE STATIC ENERGY
C     FIELD AND THEN ADD THE LOCAL RATE OF CHANGE OF STATIC ENERGY TO
C     THE EXISTING FIELD TO GET THE PROG OF THE STATIC ENERGY FIELD.
```

```
      COMMON DD(12,10,17,5),VV(12,10,17,5),U(12,10,17,5),V(12,10,17,5),
     1DIV(12,10,17,5),W(12,10,17,5),P(17),PSFC(12,10,5),DX(10),
     2Q(12,10,5),DIVZER(12,10,5),ENG(12,10,17,5),DIVBAR(10,8),
     3WBAR(10,8),ENGBAR(10,8),II,JJ,KK,LL,DY,DT,ILESS,JLESS,KLESS,LLESS,
     4IIESS,JJESS,BL,BLI,PSI,EE(12,10,17,5)
C
      DIMENSION DV11(24),DV12(24),DV13(24),X1(17),T1(5)
C
      DATA X1/' SFC',' 900',' 850',' 800',' 750',' 700',' 650',' 600',
     1' 550',' 500',' 450',' 400',' 350',' 300',' 250',' 200',' 150'/
      DATA T1/'2300','0030','0200','0330','0500'/
C
CCC
CCC   READ IN THE TITLE CARDS
CCC
C
      READ(5,198)DV11
      READ(5,199)DV12
      READ(5,197)DV13
  198 FORMAT(12A4)
  199 FORMAT(12A4)
  197 FORMAT(12A4)
C
CC    FIRST METMAP THE STATIC ENERGY FIELD
C
      DO 200 L=2,LL
      DO 200 K=3,10,7
      DO 201 J=1,JJESS
      DO 201 I=1,IIESS
  201 ENGBAR(I,J)=EE(I+1,J+1,K,L)/10.0**3
      DV11(7)=X1(K)
      DV11(10)=T1(L)
      CALL MTMPII(ENGBAR,10,8,DV11,0.004,0,0,0,0,1)
  200 CONTINUE
C
CC    NOW METMAP THE ENERGY INDEX WITHOUT PROGNOSTICATING
C
      DO 210 L=1,LL
      DO 211 J=1,JJESS
      DO 211 I=1,IIESS
  211 ENGBAR(I,J)=(EE(I+1,J+1,10,L)-EE(I+1,J+1,3,L))/10.0**3
      DV13(13)=T1(L)
      CALL MTMPII(ENGBAR,10,8,DV13,0.004,0,0,0,0,1)
  210 CONTINUE
C
CC    NOW ADD THE LOCAL RATE OF CHANGE OF STATIC ENERGY TO THE STATIC
CC    ENERGY IN ORDER TO PROG THE STATIC ENERGY ONE TIME STEP (90 MIN)
C
```

```
      DO 202 L=1,LLESS
      DO 202 K=3,10,7
      DO 203 J=1,JJESS
      DO 203 I=1,IIESS
  203 ENGBAR(I,J)=EE(I+1,J+1,K,L)/10.0**3+ENG(I+1,J+1,K,L)*1.5
      DV12(8)=X1(K)
      DV12(11)=T1(L)
      CALL MTMPII(ENGBAR,10,8,DV12,0.004,0,0,0,0,1)
  202 CONTINUE
C
CC    NOW TO METMAP THE ENERGY INDEX FIELDS AFTER PROGNOSIS
C
      DO 205 L=1,LLESS
      DO 206 J=1,JJESS
      DO 206 I=1,IIESS
  206 ENGBAR(I,J)=EE(I+1,J+1,10,L)/10.0**3+ENG(I+1,J+1,10,L)*1.5-
     1(EE(I+1,J+1,3,L)/10.0**3+ENG(I+1,J+1,3,L)*1.5)
      DV13(13)=T1(L)
      CALL MTMPII(ENGBAR,10,8,DV13,0.004,0,0,0,0,1)
  205 CONTINUE
C
      RETURN
      END
```

LIST OF REFERENCES

Browning, K. A. and F. H. Ludlam, 1962: Air flow in convective storms. Quarterly Journal of the Royal Meteorological Society, 88, 117-135.

Coleman, R. J., 1969: A diagnostic analysis of the 30 May 1967 squall line in central Oklahoma. Unpublished Master's Thesis, Naval Postgraduate School, Monterey, California, 142 pp.

Darkow, G. L., 1968: The total energy environment of severe storms. Journal of Applied Meteorology, 7, 199-205.

Fankhauser, J. C., 1969: Convective processes resolved by a mesoscale rawinsonde network. Journal of Applied Meteorology, 8, 778-798.

Fiedler, R. and H. A. Panofsky, 1970: Atmospheric scales and spectral gaps. Bulletin of the American Meteorological Society, 51, 1114-1119.

Fujita, T., 1955: Results of detailed synoptic studies of squall lines. Tellus, 7, 405-436.

Glossary of Meteorology, American Meteorological Society, 1959.

Gruber, A. and J. J. O'Brien, 1968: An objective analysis of wind data for energy budget studies. Journal of Applied Meteorology, 7, 333-338.

Inman, R. L., 1970: Operational objective analysis schemes at the national severe storms forecast center. National Severe Storms Laboratory Technical Circular 10, 50 pp.

O'Brien, J. J., 1970: Alternative solutions to the classical vertical velocity problem. Journal of Applied Meteorology, 9, 197-203.

Storm Data, 1967, Environmental Science Services Administration, 9, 75-77.

INITIAL DISTRIBUTION LIST

		No. Copies
1.	Lieutenant Commander Leo H. Craiglow, Jr. Fleet Weather Central Box 2 COMNAVMARIANAS FPO San Francisco, 96630	2
2.	Professor Ronnie L. Alberty Department of Meteorology Naval Postgraduate School Monterey, California 93940	10
3.	Professor Russel L. Elsberry Department of Meteorology Naval Postgraduate School Monterey, California 93940	1
4.	Professor George J. Haltiner Department of Meteorology Naval Postgraduate School Monterey, California 93940	1
5.	Professor Harry D. Hamilton Department of Meteorology Naval Postgraduate School Monterey, California 93940	1
6.	Professor Grant L. Darkow Department of Atmospheric Sciences University of Missouri Columbia, Missouri 65201	1
7.	Doctor Jerry D. Mahlman Geophysical Fluid Dynamics Laboratory/ESSA Princeton University, P.O. Box 308 Princeton, New Jersey 08540	1
8.	Mr. James Fankhauser National Center for Atmospheric Research Boulder, Colorado 80302	1
9.	Department of Meteorology Naval Postgraduate School Monterey, California 93940	3
10.	Library, Code 0212 Naval Postgraduate School Monterey, California 93940	2

11.	Office of the Naval Weather Service Naval Station (Washington Navy Yard Annex) Washington, D. C. 20390	1
12.	Defense Documentation Center Cameron Station Alexandria, Virginia 22314	2
13.	Officer in Charge Navy Weather Research Facility Naval Air Station, Building R-48 Norfolk, Virginia 23511	2

DOCUMENT CONTROL DATA - R & D

(Security classification of title, body of abstract and indexing annotation must be entered when the overall report is classified)

1. ORIGINATING ACTIVITY (Corporate author)

Naval Postgraduate School
Monterey, California 93940

2a. REPORT SECURITY CLASSIFICATION

UNCLASSIFIED

2b. GROUP

3. REPORT TITLE

A Mesoscale Investigation of Convective Activity

4. DESCRIPTIVE NOTES (Type of report and inclusive dates)

Master's Thesis March 1971

5. AUTHOR(S) (First name, middle initial, last name)

Leo H. Craiglow, Jr.

6. REPORT DATE	7a. TOTAL NO. OF PAGES	7b. NO. OF REFS
March 1971	90	11

8a. CONTRACT OR GRANT NO.	9a. ORIGINATOR'S REPORT NUMBER(S)
b. PROJECT NO.	
c.	9b. OTHER REPORT NO(S) (Any other numbers that may be assigned this report)
d.	

10. DISTRIBUTION STATEMENT

Approved for public release; distribution unlimited.

11. SUPPLEMENTARY NOTES	12. SPONSORING MILITARY ACTIVITY
	Naval Postgraduate School Monterey, California 93940

13. ABSTRACT

A mesoscale investigation of a series of tornadoes and thunderstorms that passed through the NSSL mesonetwork in Oklahoma, on 10 June 1967, between 1700 and 2300 CST, was conducted. Utilizing upper air data provided by NSSL, the divergence, vertical motion, and energy fields were computed.

A finite-difference technique for computing and smoothing divergence was developed. The vertical motion was then computed by means of the kinematic method. Both the total derivative and the local rate of change of static energy were computed. Using the values of the local rate of change, prognostic fields of static energy and an energy index were obtained. Finally, forecast energy indexes, divergence, and vertical motion fields were compared to the observed locations of tornadoes and thunderstorms.

14. KEY WORDS	LINK A		LINK B		LINK C	
	ROLE	WT	ROLE	WT	ROLE	WT
Mesoscale						
Tornado						
Thunderstorm						
Divergence						
Vertical Motion						
Static Energy						
Energy Index						

Thesis 126275
C783 Craiglow
c.1 A mesoscale investi-
gation of convective
activity.